UNIVERSITY OF THESSALY
SCHOOL OF ENGINEERING
DEPARTMENT OF MECHANICAL ENGINEERING

RAREFIED POLYATOMIC GAS FLOW THROUGH LONG TAPERED CHANNELS

by
KONSTANTINOS ALEXIOU

Submitted in partial fulfillment of the requirements for the degree of Diploma in Mechanical Engineering at the University of Thessaly

October, 2020

UNIVERSITY OF THESSALY
SCHOOL OF ENGINEERING
DEPARTMENT OF MECHANICAL ENGINEERING

RAREFIED POLYATOMIC GAS FLOW THROUGH LONG TAPERED CHANNELS

by
KONSTANTINOS ALEXIOU

Submitted in partial fulfillment of the requirements for the degree of Diploma in Mechanical Engineering at the University of Thessaly

October, 2020

Approved by the Committee on Final Examination:

Advisor	Dr. John Lihnaropoulos, Instructor of Applied Mathematics and Computer Science, Department of Mechanical Engineering, University of Thessaly
Member	Dr. Dimitris Valougeorgis, Professor Department of Mechanical Engineering, University of Thessaly
Member	Dr. Steryios Naris, Research Fellow Department of Mechanical Engineering, University of Thessaly

Date Approved: [02, 10, 2020]

Acknowledgements

I would like to express my special appreciation and thanks to my advisor Dr. J. Lihnaropoulos, who has been an excellent professor and helped me to do this research.

I would also like to thank Prof. D. Valougeorgis and Dr. C. Tantos for their support in this research. Both of them spent plenty of their time in order to help me comprehend many theoretical issues and resolve plenty computational difficulties that polyatomic Nitrogen mass and heat flow presented.

RAREFIED POLYATOMIC GAS FLOW THROUGH LONG TAPERED CHANNELS

KONSTANTINOS ALEXIOU

Department of Mechanical Engineering, University of Thessaly

Supervisor: Dr JOHN LIHNAROPOULOS

Instructor of Applied Mathematics and Computer Science

Abstract

The rarefied polyatomic gas flow occurs in many industrial and research applications. Typical examples are the design of gas distribution systems, vacuum pumps, micro-propulsion (in satellite maneuvering) and design of mass spectrometer. Many of these applications can be found in aerospace technology. In most of these, the dimensions of the applications are small or the pressure of gas is too low. The gas flow in this type of applications cannot be described accurately by the Navier-Stokes equations. So, the problem is described by the Boltzmann‘s equation by substituting its collision term with a reliable kinetic model. The current Thesis uses the Rykov’s kinetic model.

Rarefied gas flows appear in many applications. In the literature, the monoatomic gas flow has been studied extensively for various channel cross-sections including fixed radius and tapered channels. In contrast, the literature for polyatomic gases is limited. In the present Thesis, the gas flow in a circular cross section of a fixed radius channel and the gas flow of Nitrogen through tapered channels is being investigated. where Nitrogen is considered both as monoatomic and polyatomic molecule.

The kinetic model of Rykov demands the determination of many parameters in order to describe the flow through a circular cross section of a cylindrical tube. The value of these parameters is defined using two different methods. In the first method, the parameters stated in Rykov’s model are defined by the hypothesis that the thermal conductivity obtained by the kinetic model is close to experimental data while the value of Prandtl Number is known. However, in the second method, the value of Prandtl Number is unknown and the parameters

are determined by the same hypothesis. The results of the two methods are compared with databases for the mass and heat flow from the literature, in order to verify their validity. All databases are dimensionless, so they can be used in many dimensional cases in order to provide sufficient results for the flow of N_2.

Tapered channels are being used in many micro devices. The research of the flow of the tapered channels is investigated as a sum of many circular cross sections with different radius as the mass is preserved in every cross section. Tapered channels are being used to connect vessels with various temperatures or pressures. The results for the mass and heat flow for circular cross sections are used in order to calculate the flow of the tapered channel. In the present Thesis, the flow of Nitrogen as a monoatomic or a polyatomic molecule is being studied in tapered channels. The rarefied polyatomic gas flow through long tapered channels is also being investigated for isothermal and non-isothermal flow and for various pressure ratios, as the literature for these cases is limited.

Key words: rarefied gas dynamics, polyatomic gasses, polyatomic gas flow, tapered channels, Rykov's model, Nitrogen

ΑΡΑΙΟΠΟΙΗΜΕΝΗ ΡΟΗ ΠΟΛΥΑΤΟΜΙΚΩΝ ΑΕΡΙΩΝ ΣΕ ΚΩΝΙΚΟΥΣ ΑΓΩΓΟΥΣ ΜΕΓΑΛΟΥ ΜΗΚΟΥΣ

ΚΩΝΣΤΑΝΤΙΝΟΣ ΑΛΕΞΙΟΥ

Τμήμα Μηχανολόγων Μηχανικών, Πανεπιστήμιο Θεσσαλίας, 2020

Επιβλέπων Καθηγητής: Δρ. Ιωάννης Λυχναρόπουλος

Διδάσκων Εφαρμοσμένων Μαθηματικών και Πληροφορικής

Περίληψη

Η ροή αραιοποιημένων πολυατομικών αερίων συναντάται σε πολλές βιομηχανικές και ερευνητικές εφαρμογές. Μερικά παραδείγματα αυτών είναι ο σχεδιασμός συστημάτων διανομής αεριών, αντλιών κενού, προώθησης μικροσυσκευών (διαστημικών συσκευών) και σχεδιασμού φασματογράφων. Επίσης, μερικές από αυτές τις εφαρμογές συναντώνται στον αεροδιαστημικό τομέα. Στις περισσότερες από αυτές, οι διαστάσεις των συσκευών είναι μικρές ή η πίεση που χαρακτηρίζει το αέριο είναι μικρή. Η ροή του αερίου σε αυτού του είδους τις εφαρμογές δεν μπορεί να περιγραφεί με ακρίβεια από τις εξισώσεις Navier-Stokes. Σαν αποτέλεσμα, η περιγραφή αυτών των προβλημάτων γίνεται με την χρήση της εξίσωσης του Boltzmann υποκαθιστώντας τον όρο που αφορά τις συγκρούσεις με ενός αξιόπιστου κινητικού μοντέλου. Στην παρούσα διπλωματική εργασία χρησιμοποιείται το κινητικό μοντέλο του Rykov.

Η αραιοποιημένη ροή αερίων συναντάται σε πολλές εφαρμογές. Στην βιβλιογραφία, έχει γίνει εκτενής μελέτη της ροής αερίων ως μονοατομικά για ποικίλες διατομές περιλαμβάνοντας τους αγωγούς σταθερής διατομής και τα κωνικά κανάλια. Αντίθετα, η βιβλιογραφία για ροές πολυατομικών αερίων είναι περιορισμένη. Στην παρούσα διπλωματική εργασία, μελετάται η ροή αερίων σε μία τυχαία κυκλική διατομή ενός αγωγού και η ροή του Αζώτου μέσω κωνικών αγωγών, όπου το Άζωτο θεωρείται τόσο ως μονοατομικό όσο και ως πολυατομικό μόριο.

Το κινητικό μοντέλο του Rykov απαιτεί τον προσδιορισμό αρκετών παραμέτρων προκειμένου να μπορεί να περιγραφεί η ροή διαμέσου μια τυχαίας διατομής ενός κυκλικού

αγωγού. Ο καθορισμός αυτών των παραμέτρων γίνεται με δύο μεθόδους. Στην πρώτη μέθοδο, ο καθορισμός των παραμέτρων του μοντέλου του Rykov γίνεται υποθέτοντας πως η θερμική αγωγή του κινητικού μοντέλου είναι ίδια με τα πειραματικά δεδομένα με την τιμή του αριθμού Prandtl να είναι γνωστή. Αντίθετα, στην δεύτερη μέθοδο, η τιμή του Prandtl δεν είναι γνωστή και ο καθορισμός των παραμέτρων πραγματοποιείται χρησιμοποιώντας την ίδια υπόθεση. Τα αποτελέσματα που προκύπτουν από τις δύο μεθόδους συγκρίνονται με δεδομένα που αφορούν την ροή μάζας και θερμότητας από την βιβλιογραφία προκειμένου να αποδειχθεί η ορθότητα τους. Όλα τα παραπάνω αποτελέσματα είναι αδιάστατα και μπορούν να χρησιμοποιηθούν στην μελέτη ροής αερίου N_2 σε αγωγούς διαφόρων διαστάσεων.

Οι κωνικοί αγωγοί χρησιμοποιούνται σε πολλές μικροσυσκευές. Η μελέτη της ροής ενός κωνικού αγωγού μελετάται ως ένα σύνολο κυκλικών διατομών διαφορετικής ακτίνας όπου η μάζα διατηρείται σταθερή. Οι κωνικοί αγωγοί χρησιμοποιούνται για να συνδέσουν δοχεία με διάφορες θερμοκρασίες ή πιέσεις. Τα αποτελέσματα της ροής μάζας και θερμότητας κυκλικών διατομών χρησιμοποιούνται για να υπολογισθεί η ροή σε ένα κωνικό αγωγό. Στην παρούσα πτυχιακή εργασία, η ροή αζώτου ως μονοατομικό ή πολυατομικό αέριο μελετάται για τους κωνικούς αγωγούς. Στην παρούσα διπλωματική εργασία μελετώνται επίσης ροές αραιοποιημένου πολυατομικού αερίου σε αγωγούς μεταβλητής διατομής για ισοθερμοκρασιακή και μη ισοθερμοκρασιακή ροή για ποικίλους λόγους πίεσης, καθώς δεν υπάρχει εκτεταμένη έρευνα στην υπάρχουσα βιβλιογραφία.

Λέξεις-κλειδιά: δυναμική αεροποιημένου αερίου, πολυατομικά αέρια, ροή πολυατομικού αερίου, κωνικά κανάλια, μοντέλο του Rykov, Άζωτο

Contents

LIST OF TABLES

LIST OF FIGURES

Chapter 1. INTRODUCTION

The rarefied gas flow has attracted the interest of many researchers due to its importance in many industrial and research applications. These gas flows appear in small dimension devices or in applications where the pressure is low. The flow cannot be described by the Navier-Stokes' equations accurately, so the Boltzmann's equation is selected to describe the flow by substituting its collision term with a reliable kinetic model, in the current Thesis with Rykov's kinetic model.

The investigation of rarefied gas flow on monoatomic gases has been mainly based either on the linearized Boltzmann's equation [9] or on kinetic models named Bhatnagas-Gross-Krook [3] and Shakhov [33]. The polyatomic gases have not been investigated extensively in the literature due to their complexity.

In the literature, there is extensive investigation for different cross sections. Parallel plates have been researched for both monoatomic (Ohwada[5], Sharipov and Seleznev[6]) and polyatomic gases (Loyalka and Storvick[7]). Furthermore, long and short circular and elliptic tubes (Sharipov[34], Graur and Sharipov[35], Alexeenko[36] and Pantazis[37]), long rectangular, triangular and trapezoidal cross sections (Sharipov[38] and Ritos[39]) have been investigated in the literature.

Rarefied monoatomic gas flows based on Rykov's model have been extensively investigated in the past. Monoatomic gas flows have been researched for both fixed radius circular tube and variable circular radius tubes (Sharipov and Bertoldo[30]) . For polyatomic gas flow in fixed radius circular tube, there is an extensive research by Loyalka[8] and Tantos[29].

In the present Thesis, the rarefied gas flow for both monoatomic and polyatomic gases in a circular cross section of a circular tube is investigated, using two different methods. The investigation of monoatomic and polyatomic gas flow through a long tapered channel demands the research of mass and heat flow in circular cross sections.

1.1 General concepts

The pressure-driven flow and the thermal flow through long diverging or converging channels, has attracted the scientific attention of many researchers. This happens due to its presence in many technological applications including vacuum technology, high altitude aerodynamics, pumping and leak detection. In the aerospace technology, a lot of researchers focus on satellite propulsion and maneuvering of spacecrafts. In the diode effect, where the inlet and the outlet are the same, the mass flow is lower when the flow is in the diverging direction compared to a converging channel. This phenomenon is significant, especially in micro devices.

In the present Thesis, there is an investigation for the rarefied monoatomic and polyatomic gas flow in a circular cross section of fixed radius tube. The investigation of monoatomic and polyatomic non-dimensional gas flow for long tapered is based on this database.

1.2 Content and Structure

In Chapter 2, the polyatomic kinetic problem and the kinetic models required to solve the Boltzmann equation numerically are introduced. Following that, there is an extensive description of Holway's and Rykov's models.

In Chapter 3, the pressure and temperature driven polyatomic flow through long tubes is introduced. Two reservoirs, with different pressure and temperature, are connected with a long fixed-radius tube. Based on this model, the flow through a circular cross section of the tube is researched. The results of the flow in circular cross section, for different rarefaction parameters and temperatures, are used in order to investigate the flow for long tapered channels both for monoatomic and polyatomic gases (N_2). In order to research the gas flow, the Boltzmann equation is needed to be linearized for long tubes.

In Chapter 4, in order to specify the mass and heat flow through a circular cross section of a long tube, some parameters for Rykov's model that are used in order to determine the flow of N_2 should be specified. Two methods are used for the definition of these parameters. In the first method, the value of the Prandtl Number is known from the literature [27] and the parameters ω_0 and ω_1 are defined from a system of equations, either eq. (2.4) or eq. (2.5) from Mason and Monchick [1] and eq. (2.6) from Rykov [11]. In this Thesis eq. (2.4) is used.

On the contrary, in the second method the parameters are specified from [10] and the theoretical value of Prandtl number is calculated by eq. (2.6) from [11].

In Chapter 5, the databases of Chapter 4 are being verified. So, the results calculated of mass and heat flow are being compared with results from literature. In addition, the databases of bibliography, which are the same with the results of Chapter 4, are used in order to specify the flow of N_2 in a tapered channel. The flow, for different pressure ratios between inlet and outlet of the channel, is researched both as isothermal and non-isothermal. In the first case it is assumed that Nitrogen is a monoatomic, where in the second case it is a polyatomic gas. All the results are being verified by data from bibliography.

1.3 Contribution of this research

All the results that occurred in this Thesis can be used in many scientific researches. Both the codes and the databases that were developed and investigated in this Thesis can be used in order to specify the flow of many gases through long tubes and tapered channels in micro vacuums. Furthermore, this research concludes that the mass and heat flow in both methods are the same. These methods had been used in order to specify some parameters of the flow. The results of the two methods can be used in order to validate and calculate the flow for dimensional gas flows for a variety of temperatures, pressures, dimensions and rarefaction parameters for both theoretical and real conditions experiments. The database of rarefied polyatomic gas flow in tapered channels which is investigated in this Thesis based on Rykov's model is valuable for the current scientific literature as future research can be based upon it.

Chapter 2. POLYATOMIC KINETIC MODEL

2.1 Introduction to polyatomic kinetic modeling

The solution to Boltzmann's equation, either numerical or analytical, needs great computational effort. This effort can be reduced substituting with a reliable kinetic model, the term of collision number. Reliable kinetic models can be the Holway [12], Hanson and Morse [13], Brau [4], Wood [14], McCormack [15], Rykov [16], Andries [17], Marques [18] and Fernandes and Marques [19].

In the Holway's model, the kinetic equations have been obtained by the employment of the diagonal approximation in the linear operator of the Boltzmann's equation for diatomic gases. The Hanson and Morse model is similar to Holway's model but it does not satisfy the requirements in every state. Furthermore, in Morse's model, it is stated that heat capacity at constant volume and at all degrees of freedom is independent from the temperature only for high temperatures. In Brau's model, the elastic collisions are treated by a single relaxation-time term and the inelastic collisions are described by a FokkerPlanck term. The Wood model is an ellipsoidal statistical model which allows the calculation of the correct value of the Prandtl number of the gas. The model proposed by McCormack is an extension based on the model described by Hanson and Morse. The Rykov model can be written as Holway's model and consists of two components, the elastic and inelastic collisions. A detailed analysis of Rykov's model follows in paragraph 2.2. The model provided by Andries, provides correct expression of viscosity and thermal conductivity coefficients. In Marques work, the replacement of Boltzann's collision operator by a single relaxation-time term states its kinetic model equation for polyatomic gases. The Fernandes and Marques model is similar to the model by Marques but the collision operator is replaced by a single relaxation-time term with Grads 6-moment. The disadvantage of this model is, that it is valid for some cases in which the energy exchange of translational and internal degrees of freedom is slow. The Wood, McCormack, Marques and Fernandes and Marques belong to linearized kinetic theory models. In the past, it was proved that the Holway, Andries and Rykov models provide results similar to experimental data. This is the reason for selecting Rykov's model in the present Thesis.

2.2 Elastic and inelastic collision terms in models

In rarefied polyatomic gas flows and heat transfer problems, the use of Holway's or Rykov's problem has been applied with significant success. In a one-dimensional heat transfer problem, the models of Holway and Rykov can be described in a similar form.

$$\xi_y \frac{\partial \hat{L}}{\partial \hat{y}} = \frac{\widehat{P_{tr}}}{\mu_{tr}} Pr^{\chi} \left[\left(1 - \frac{1}{Z^{(i)}}\right) \left(\hat{L}_{tr}^{(i)} - \hat{L}\right) + \frac{1}{Z^{(i)}} \left(\hat{L}_{rot}^{(i)} - \hat{L}\right) \right] \tag{2.1}$$

where $i = H$ for the model of Holway and $i = R$ for the model of Rykov. In the right hand of the eq. (2.1), the pressure is defined only by the translational temperature, $\hat{P}_{tr} = nk_B T_{tr}$. The $\mu_{tr} = \mu(T_{tr})$ is the viscosity of gas which is also defined only by the translational temperature. The term of Pr is for the Prandl number and the parameter χ, where $\chi = 1$ for the model of Holway and $\chi = 0$ for the model of Rykov respectively. The parameter $Z^{(i)}$ is the fraction of rotational collisions of the total number and its value is between 0 and 1. The first two terms of the right side of q. (2.1) describes the elastic collisions, which conserves the translational energy of molecules and inelastic collisions which exchanges the rotational and the translational energies respectively.

The $\hat{L} = \left[\hat{g}, \hat{h}\right]^T$ vector describes the unknown distribution functions and depends on the velocity vector of molecules $\upsilon = (\xi_\chi, \xi_y, \xi_z)$ and spatial variable $\hat{y}$. Also, on the right side of the Eq. (2.1), are the translational distribution function $\hat{L}_{tr}^{(i)} = \left[\hat{g}_{tr}^{(i)}, \hat{h}_{tr}^{(i)}\right]^T$ and the rotational distribution function $\hat{L}_{rot}^{(i)} = \left[\hat{g}_{rot}^{(i)}, \hat{h}_{rot}^{(i)}\right]^T$ where their parameters are analyzed bellow:

- **Holway kinetic model (Eq. 2.2)**

$$\hat{g}_{tr}^{(H)} = n \left(\frac{m}{2\pi k_B T_{tr}}\right)^{3/2} exp\left(\frac{-mu^2}{2k_B T_{tr}}\right) \tag{2.2a}$$

$$\hat{h}_{tr}^{(H)} = \frac{jk_B T_{rot}}{2} \hat{g}_{tr}^{(H)} \tag{2.2b}$$

$$\hat{g}_{rot}^{(H)} = n \left(\frac{m}{2\pi k_B T}\right)^{3/2} exp\left(\frac{-mu^2}{2k_B T}\right) \tag{2.2c}$$

$$\hat{h}_{rot}^{(H)} = \frac{jk_B T}{2} \hat{g}_{rot}^{(H)} \tag{2.2d}$$

- **Rykov kinetic model (Eq. 2.3)**

$$\hat{g}_{tr}^{(R)} = \hat{g}_{tr}^{(H)} \left[1 + \frac{2}{15} \frac{mQ_{tr}\xi_y}{n(kT_{tr})^2} \left(\frac{mu^2}{2k_B T_{tr}} - \frac{5}{2}\right)\right] \tag{2.3a}$$

$$\hat{h}_{tr}^{(R)} = \hat{g}_{tr}^{(H)} k_B T_{rot} \left[1 + \frac{2}{15}\frac{mQ_{tr}\xi_y}{n(k_B T_{tr})^2}\left(\frac{mu^2}{2k_B T_{tr}} - \frac{5}{2}\right) + (1-\kappa)\frac{mQ_{rot}\xi_y}{nk_B^2 T_{tr} T_{rot}}\right] \quad (2.3b)$$

$$\hat{g}_{rot}^{(R)} = \hat{g}_{rot}^{(H)}\left[1 + \omega_0 \frac{2}{15}\frac{mQ_{tr}\xi_y}{n(k_B T)^2}\left(\frac{mu^2}{2k_B T} - \frac{5}{2}\right)\right] \quad (2.3c)$$

$$\hat{h}_{rot}^{(R)} = \hat{g}_{rot}^{(H)} k_B T\left[1 + \omega_0 \frac{2}{15}\frac{mQ_{tr}\xi_y}{n(k_B T)^2}\left(\frac{mu^2}{2k_B T} - \frac{5}{2}\right) + \omega_1(1-\kappa)\frac{mQ_{rot}\xi_y}{n(k_B T)^2}\right] \quad (2.3d)$$

On the eqs. (2.3), the parameter $\kappa = \mu/(mnD)$ is a constant where the value is 1/1.2 for hard spheres and 1/1.543 for Maxwell molecules [22] or somewhere between these two values. On the next chapter, in order to investigate the flow in long channels, the parameter κ is being chosen from the hard spheres' model. The parameters ω_0 and ω_1 can either be defined from bibliography or using the theory in [10]. Using this theory, the value of rotational collision number $Z^{(R)}$ can be defined through the value of parameter Z_{rot}. The parameters ω_0 and ω_1 can be defined from the eqs. (2.4), (2.5) and (2.6) by [10], [11]:

$$\left(1 + \frac{1-\omega_0}{2Z^{(R)}}\right)^{-1} = 1 - \frac{1}{2Z^{(R)}}\left(1 - \frac{2}{5\kappa}\right) \quad (2.4)$$

$$\left(1 + \frac{(1-\kappa)(1-\omega_1)}{Z^{(R)}\kappa}\right) = 1 + \frac{3}{4Z^{(R)}}\left(1 - \frac{2}{5\kappa}\right) \quad (2.5)$$

Prandtl number depends on the characteristics of fluid or gas. Its equation is given by [11]:

$$Pr = \frac{7}{5Z^{(R)}}\left[\frac{3}{2Z^{(R)} + 1 - \omega_0} + \frac{0.4}{\kappa Z^{(R)} + (1-\kappa)(1-\omega_1)}\right]^{-1} \quad (2.6)$$

which derives from the equations (2.4) and (2.5).

In this equation, Prandtl number depends on κ, $Z^{(R)}$, ω_0 and ω_1.

In the current Thesis, for the determination of the parameters (ω_0 and ω_1) two different methods are used. In the first method, the value of the two parameters is specified using eqs. (2.4) and (2.5) which is independent from the temperature and the value of Prandtl number of the gas. In the second method, the temperature's value is known and so is the

value of Prandtl number. But for the investigation of the mass flow and heat flow, the value of the parameters ω_0 and ω_1 is needed to be determined. This occurs by specifying the value of the parameters ω_0 and ω_1 through eq. (2.6) and eqs. (2.4) or (2.5). The comparison of the results of the two methods concludes in the fact that dimensionless results are the same. In both methods, the values of κ and $Z^{(R)}$ are given. It should be mentioned that eqs (2.4) and (2.5) derive from [10] and eq. (2.6) from [11] as a combination of eqs. (2.4) and (2.5).

Chapter 3. POLYATOMIC FLOWS THROUGH LONG TUBES

In this chapter, there is an extensive analysis of the problem that is being solved in order to specify the flow in a circular cross section. In order to specify the rarefied gas flow in a circular tube, the parameters and the conditions of the problem are needed to be specified. There are two reservoirs which are connected with a long tube with different temperature and pressure conditions. The solution of the problem requires the linearization of the kinetic model (Rykov) that is being used. Also, a case is mentioned, where the flow due to pressure difference is opposite to the flow due to temperature difference and as result, the total mass flow is zero.

3.1 Pressure and temperature driven polyatomic flow through long tubes

Two large reservoirs A and B are connected with a long circular tube of radius R. In reservoir A the conditions are T_A for temperature and P_A for pressure. In reservoir B, the temperature and pressure are T_B and P_B respectively. The temperature and pressure are constant in both reservoirs and their values are given. The correlation of pressure A and B is $\hat{P}_A < \hat{P}_B$ and the correlation of temperature A and B is $\hat{T}_A > \hat{T}_B$. In addition, the differences between pressures and temperatures of reservoirs A and B are too small.

$$\hat{P}_B - \hat{P}_A \ll \frac{\hat{P}_A + \hat{P}_B}{2} \tag{3.1}$$

$$\hat{T}_B - \hat{T}_A \ll \frac{\hat{T}_A + \hat{T}_B}{2} \tag{3.2}$$

When the two reservoirs are connected, with different temperatures and same pressure, the polyatomic gas flows from the cold reservoir ($\hat{T}_B$) to the hot one ($\hat{T}_A$). This is called thermal creep flow. If the whole system is closed, then there is a drop of pressure between the two reservoirs. The polyatomic flow is opposite to the thermal creep due to the pressure drop. This phenomenon is called thermomolecular pressure effect and it is mainly seen in monoatomic gases flows. It is also assumed that the length of the tube is much bigger than its radius ($R \ll \mathrm{L}$). In this study, the thermal creep flow and the thermomolecular pressure effect phenomenon is being investigated for the flow of polyatomic gases through long circular tubes.

3.2 Linearization for long tubes

There are small temperature and pressure differences between the two ends of the long circular tube. Also, according to the correlation of radius and length of the tube, the flow is considered fully developed without end effects in the inlet and outlet of tube. As a result, the equations of the problem can be linearized and are defined by the eqs. (3.3) and (3.4) from [21] and [22]:

$$\hat{g} = \hat{f}_w^{(M)}(1 + L) \tag{3.3}$$

$$\hat{h} = \frac{j}{2} k_B T_w \hat{f}_w^{(M)}(1 + H) \tag{3.4}$$

where: $\hat{f}_w^{(M)} = n_w \left(\frac{m}{2\pi k_B T_w}\right)^{3/2} exp\left(\frac{-mu^2}{2k_B T_w}\right)$

The L and H are linearized distribution functions which are unknown. Both L and H depend on radial spatial coordinate $\hat{r}$ ($0 \leq \hat{r} \leq R$) and the molecular velocity vector (cylindrical coordinates) $u = (\xi cos\theta, \xi sin\theta, \xi z)$ with $\theta = \tan^{-1}\left(\frac{\xi_y}{\xi_x}\right)$, $L(\hat{r}, u)$, and $H(\hat{r}, u)$. The two former equations are independent from the z-coordinate. In the local-Maxwellian function $\hat{f}_w^{(M)}$, there is the $\hat{z}$-dependence. At each cross section, the rotational T_{rot}, translational T_{tr} and local temperature T is equal to T_W. Also, the temperature T_w, the number density n_w and the pressure $\hat{P}_w = n_w k_B T_w$ are constant in each cross section of the tube.

According to [21], [22], [23] the unknown equations of L and H can be defined by the equations:

$$\xi \cos\theta \frac{\partial L}{\partial \hat{r}} - \frac{\xi \sin\theta}{\hat{r}} \frac{\partial L}{\partial \theta} = u(L_0 - L) - \xi_z \frac{dln\hat{P}_w}{d\hat{z}} - \xi_z \left(\frac{mu^2}{2k_B T_w} - \frac{5}{2}\right) \frac{dlnT_w}{d\hat{z}} \tag{3.5a}$$

$$\xi \cos\theta \frac{\partial H}{\partial \hat{r}} - \frac{\xi \sin\theta}{\hat{r}} \frac{\partial H}{\partial \theta} = u(H_0 - H) - \xi_z \frac{dln\hat{P}_w}{d\hat{z}} - \xi_z \left(\frac{mu^2}{2k_B T_w} - \frac{3}{2}\right) \frac{dlnT_w}{d\hat{z}} \tag{3.5b}$$

$$L_0 = 2\frac{m\xi_z \hat{u}_z}{2k_B T_w} + \left(\frac{\omega_0 - 1}{Z} + 1\right) \frac{2}{15} Q_{tr} \frac{m\xi_z}{\hat{P}_w k_B T_w} \left(\frac{mu^2}{2k_B T_w} - \frac{5}{2}\right) \tag{3.5c}$$

$$H_0 = 2\frac{m\xi_z \hat{u}_z}{2k_B T_w} + \left(\frac{\omega_0 - 1}{Z} + 1\right) \frac{2}{15} Q_{tr} \frac{m\xi_z}{\hat{P}_w k_B T_w} \left(\frac{mu^2}{2k_B T_w} - \frac{5}{2}\right) + \left(\frac{\omega_1 - 1}{Z} + 1\right)(1 - \kappa) Q_{rot} \frac{2m\xi_z}{j\hat{P}_w k_B T_w} \tag{3.5d}$$

In the eqs. (3.5), the term $u = \hat{P}_w / \mu(T_w)$ is the collision frequency. The viscosity $\mu(T_w)$ is at temperature T_w. The parameter Z^{-1} describes the rotational degrees of the rotational collisions of their total number. The parameter j indicates the rotational degrees of

freedom and its value is 2 or 3 for linear and nonlinear polyatomic molecules. The parameters ω_0 and ω_1 need to be defined as described in Chapter 3 by eqs. (2.4) and (2.5) in order to obtain the correct values of translational and rotational thermal conductivity coefficients. Furthermore, the parameter $\kappa = \mu/(mnD)$ is constant and its value is 1/1.2 for hard spheres and 1/1.543 for Maxwell molecules. In the eq. (3.5) the terms of velocity $\hat{u}_z$, the translational heat flux Q_{tr} and the rotational heat flux Q_{rot} need to be analyzed and defined as functions with the functions of L and H. The equations are defined as:

$$\hat{u}_z(\hat{r}) = \frac{1}{n_w}\int_{-\infty}^{\infty}\int_0^{2\pi}\int_0^{\infty} \xi\xi_z \hat{f}_w^{(M)} L d\xi d\theta d\xi_z \tag{3.6}$$

$$Q_{tr}(\hat{r}) = \frac{m}{2}\int_{-\infty}^{\infty}\int_0^{2\pi}\int_0^{\infty} \xi\xi_z \left(u^2 - \frac{5k_B}{m}T_w\right) \hat{f}_w^{(M)} L d\xi d\theta d\xi_z \tag{3.7}$$

$$Q_{rot}(\hat{r}) = \frac{jk_BT_w}{2}\int_{-\infty}^{\infty}\int_0^{2\pi}\int_0^{\infty} \xi\xi_z \hat{f}_w^{(M)} (L-H) d\xi d\theta d\xi_z \tag{3.8}$$

In eqs (3.6), (3.7) and (3.8), m is the molecular mass and k_B is the Boltzmann constant and all of them apply in each cross section of the tube.

For a certain cross section $\hat{z} = \hat{z_0}$ of the long cylindrical tube, the non-dimensional quantities are defined as:

$$r = \frac{\hat{r}}{R} \quad (3.9a)\ ,\ \zeta = \frac{\xi}{u_0}\ (3.9b)\ ,\ c_z = \frac{\xi_z}{u_0}\ (3.9c)\ ,\ \hat{f}_w^{(M)} = \frac{\hat{f}_w^{(M)} u_0^3}{n_0}\ (3.9d)$$

$$u_z = \frac{\hat{u}_z}{u_0}\ (3.9e)\ ,\ q_{tr} = \frac{Q_{tr}}{\hat{P}_0 u_0}\ (3.9f)\ ,\ q_{rot} = \frac{Q_{rot}}{\hat{P}_0 u_0} \quad (3.9e)$$

where u_0 is the probable molecular speed and $\hat{P}_0$ is the reference pressure. The equations of probable molecular speed and reference pressure are described as:

$$u_0 = \sqrt{2k_BT_0/m}\ \ ,\hat{P}_0 = n_0 k_B T_0\ \ ,n_0 = n_w\ ,T_0 = T_w\ ,\ \hat{P}_0 = \hat{P}_w$$

The problem needs to be simplified, so that parameter c_z can be replaced. For this simplification, the integrals are introduced:

$$F = \frac{1}{\sqrt{\pi}}\int_{-\infty}^{\infty} L c_z exp(-c_z^2) dc_z \tag{3.10}$$

$$G = \frac{1}{\sqrt{\pi}}\int_{-\infty}^{\infty} L {c_z}^3 exp(-c_z^2) dc_z \tag{3.11}$$

$$S = \frac{1}{\sqrt{\pi}}\int_{-\infty}^{\infty} H c_z exp(-c_z^2) dc_z \tag{3.12}$$

All the equations of the system of eqs. (3.5) can be rewritten, using the eqs. (3.10), (3.11) and (3.12) as:

$$\xi\cos\theta\frac{\partial F}{\partial r} - \frac{\xi\sin\theta}{r}\frac{\partial F}{\partial\theta} = \delta_0(F_0 - F) - \frac{1}{2}[X_P + (\xi^2 - 1)X_T] \tag{3.12a}$$

$$\xi \cos\theta \frac{\partial G}{\partial r} - \frac{\xi \sin}{r}\frac{\partial G}{\partial \theta} = \delta_0(G_0 - G) - \frac{3}{4}(X_P + \xi^2 X_T) \quad (3.12b)$$

$$\xi \cos\theta \frac{\partial S}{\partial r} - \frac{\xi \sin\theta}{r}\frac{\partial S}{\partial \theta} = \delta_0(S_0 - S) - \frac{1}{2}(X_P + \xi^2 X_T) \quad (3.12c)$$

$$F_0 = u_z + \left(\frac{\omega_0 - 1}{Z} + 1\right)\frac{2}{15} q_{tr}(\xi^2 - 1) \quad (3.12d)$$

$$G_0 = \frac{3u_z}{2} + \left(\frac{\omega_0 - 1}{Z} + 1\right)\frac{1}{5} q_{tr}\xi^2 \quad (3.12e)$$

$$S_0 = u_z + \left(\frac{\omega_0 - 1}{Z} + 1\right)\frac{2}{15} q_{tr}(\xi^2 - 1) + \left(\frac{\omega_1 - 1}{Z} + 1\right)(1 - \kappa)\frac{2q_{rot}}{j} \quad (3.12f)$$

where the u_z, q_{tr}, δ_0 and q_{rot} are defined as:

$$u_z = \frac{1}{\pi}\int_0^{2\pi}\int_0^{\infty} \xi F exp(-\xi^2) d\xi d\theta \quad (3.13)$$

$$q_{tr} = \frac{1}{\pi}\int_0^{2\pi}\int_0^{\infty} \xi \left[F\left(\xi^2 - \frac{5}{2}\right) + G\right] exp(-\xi^2) d\xi d\theta \quad (3.14)$$

$$q_{rot} = \frac{j}{2\pi}\int_0^{2\pi}\int_0^{\infty} \xi (S - F) exp(-\xi^2) d\xi d\theta \quad (3.15)$$

$$\delta_0 = \frac{\hat{P}_0 R}{\mu_0 u_0} \quad (3.16)$$

and the parameters of dimensionless pressure X_P and dimensionless temperature X_T are described as:

$$X_P = \frac{R\, d\hat{P}_w}{\hat{P}_w\, d\hat{z}} \quad (3.17a)$$

$$X_T = \frac{R\, dT_w}{T_w\, d\hat{z}} \quad (3.17b)$$

The total heat flux is $\mathrm{q} = q_{tr} + q_{rot}$.

The interaction between the wall and the gas molecules is modeled by a diffuse-specular reflection condition as described in [23].

On the boundaries of the system, on the wall, the equation that relates the particles which arrive and depart is described as:

$$\hat{g}^+ = a_M \hat{f}_w^{(M)} + (1 - a_M)\hat{g}^- \quad (3.18a)$$

$$\hat{h}^+ = a_M \frac{j}{2} k_B T_B \hat{f}_w^{(M)} + (1 - a_M)\hat{h}^- \quad (3.18b)$$

where $\hat{g}^+$, $\hat{h}^+$ are the distributions representing particles which depart from the wall and $\hat{h}^+$, $\hat{h}^-$ are the distributions representing particles which arrive at the wall. The parameter a_M is the tangential momentum accommodation coefficient and characterizes the portion of particles which are reflected from the wall. Furthermore, $\hat{f}_w^{(M)}$is the Maxwellian and its value is defined by the temperature of the wall.

The boundary conditions need to be specified. So, applying nondimensionalization, linearization and projection for the wall boundaries for $r = 1$, the distribution functions F, G and S are simplified as:

$$F^{+}(1,\zeta,\theta) = (1-a_M) \quad F^{-}(1,\zeta,\pi-\theta) \tag{3.20a}$$

$$G^{+}(1,\zeta,\theta) = (1-a_M) \quad G^{-}(1,\zeta,\pi-\theta) \tag{3.20b}$$

$$S^{+}(1,\zeta,\theta) = (1-a_M) \quad S^{-}(1,\zeta,\pi-\theta) \tag{3.20c}$$

In contrast to the eqs. (3.20), for $r = 0$, in the middle of the cross section of the long cylindrical tube, the distribution functions F, G and S are described as:

$$F^{+}(0,\zeta,\theta) = F^{-}(0,\zeta,\pi-\theta) \tag{3.21a}$$

$$G^{+}(0,\zeta,\theta) = G^{-}(0,\zeta,\pi-\theta) \tag{3.21b}$$

$$S^{+}(0,\zeta,\theta) = S^{-}(0,\zeta,\pi-\theta) \tag{3.21c}$$

The boundary conditions of eqs. (3.20) are valid for $\theta \in [\pi/2, 3\pi/2]\ or\ r = 1$. In addition, the eqs. (3.21) are valid for $\theta \in [-\pi/2, \pi/2]\ or\ r = 0$.

In system of eqs. (3.12) the linear integrodifferential equation is described in addition with corresponding macroscopic quantities, eqs. (3.13), (3.14) and (3.15). Also, the boundary conditions and their numerical solutions are added in the system, eqs. (3.20) and (3.21).

The kinetic solution of gas flow in cylindrical tube needs the specification of parameters κ, ω_0 and ω_1 as described in Chapter 2 in eqs. (2.4), (2.5) and (2.6). Furthermore, the rarefaction parameters δ_0, the accommodation coefficient α_M and the parameter Z need to be defined before the solution.

The dimensionless mass flow rate (W) and heat flow rate (E) are defined as:

$$W = \frac{\dot{M}u_0}{\pi R^2 \hat{P}_0} = 4\int_0^1 u_z r dr \tag{3.22}$$

$$E = \frac{2\dot{E}}{\pi R^2 \hat{P}_0 u_0} = 4\int_0^1 q r dr \tag{3.23}$$

with $\dot{M}$ and $\dot{E}$ being the dimensional mass flow and the dimensional heat flow respectively. In research of polyatomic gas, the dimensional heat flow (E) is a sum of the heat related to translational degrees of freedom (E_{tr}) and the heat related to rotational degrees of freedom (E_{rot}). In extremely high temperatures, this sum is affected by the vibration of the gas particles.

$$E_{tr} = 4\int_0^1 q_{tr} r dr \tag{3.24a}$$

$$E_{rot} = 4\int_0^1 q_{rot} r dr \tag{3.24b}$$

$$E = E_{tr} + E_{rot} \tag{3.24c}$$

where q_{tr} and q_{rot} are defined in eqs. (3.14) and (3.15).

As it is described in Chapter 2, the flow rate of mass and heat can be split in two dividends, because of the small differences in temperature and pressure between both ends of the long cylindrical tube.

$$\mathrm{W} = -W_P X_P + W_T X_T \tag{3.25a}$$

$$\mathrm{E} = E_P X_P - E_T X_T \tag{3.25b}$$

$$E_P = E_{tr,P} + E_{rot,P} \tag{3.25c}$$

$$E_T = E_{tr,T} + E_{rot,T} \tag{3.25d}$$

The thermal creep flow problem is solved by replacing the terms X_P= 0 and X_T= 1 in eqs. (3.25). The coefficients W_P, $E_{tr,P}$ and $E_{rot,P}$ do not participate in the solution of the problem while only W_T, $E_{tr,T}$ and $E_{rot,T}$ participate in the solution. The Poiseuille problem is being solved when X_P= 1 and X_T= 0. The only terms obtained in this solution are W_P, $E_{tr,P}$ and $E_{rot,P}$. The eq. (3.26) is used in order to verify the results of the calculations. According to Onsager's relation [21], in the Poiseuille problem the mass flow rate due to the temperature is equal to the heat flow due to the pressure.

$$W_T = E_P \tag{3.26}$$

3.3 Thermomolecular pressure effect

The thermomolecular pressure effect is extremely significant in flow studies. In practice, this method is used in order to calculate the pressure of a reservoir B when its temperature is constant, T_B and the temperature T_A and pressure $\hat{P}_A$ are known for the reservoir A which is connected with the tube.

Maxwell [24] explained this phenomenon theoretical, while Knudsen [25] continued the investigation of the thermomolecular pressure effect based on Reynold's study [26].

The equation that is used in order to correlate the terms of pressure and temperature of reservoir A, T_A and $\hat{P}_A$ and pressure and temperature of reservoir A, T_B and $\hat{P}_B$ is:

$$\frac{\hat{P}_B}{\hat{P}_A} = \left(\frac{T_B}{T_A}\right)^{\gamma} \tag{3.27}$$

where:

$$\gamma = \frac{W_T}{W_P} \tag{3.28}$$

with W_T being the mass flow due to temperature and W_P being the mass flow due to pressure. In order to specify accurately the coefficient γ, the sum of mass flow is set to zero, $W = 0$. The coefficient parameter γ depends on many other parameters which are related with the characteristics of gas and the tube. Coefficient γ depends on rarefaction parameter δ_0, length-to-radius ratio of the tube, the nature of the gas-surface interaction and the type of the gas.

Chapter 4 FULLY DEVELOPED GAS FLOW THROUGH LONG TUBE

The specification of mass and heat flow is based on the solution of kinetic model of Rykov which was analytically described in Chapter 2. In order to define the flows in a fixed-radius channel, the parameters of the gas, κ, $Z^{(R)}$, ω_0 and ω_1 need to be specified. In this chapter, these parameters are determined by following two different methods. Both in first and in the second method, the parameters κ and $Z^{(R)}$ have the same value. In contrast, the other two parameters are defined using two different methods. In the second method, the parameters ω_0 and ω_1 are being specified from the eqs. (2.4) and (2.5) while in the first method a different approach is used. The temperatures are chosen in advance and thus the value of the Prandtl number of the gas is also determined. The value of the parameter ω_0 is specified from the eq. (2.4) and the value of parameter ω_1 is defined through the value of Prandtl number.

4.1 Flow rate and thermomolecular pressure effect analysis

The solution of mass and heat flow in long cylindrical tubes needs the definition of many parameters, both for the characteristics of tube and for the characteristics of gas. The rarefaction parameter δ_0, the parameters κ, $Z^{(R)}$, ω_0, ω_1, the rotational degrees of freedom j and the tangential momentum accommodation coefficient α_M need to be defined.

In paragraph 4.2, various values for parameter δ_0 between 0.01 and 50 are used, the parameter $Z^{(R)}$ is defined analytically in the next sub-chapter according to Bird 's theory and the parameters κ, ω_0 and ω_1 are replaced by the values from the eqs. (2.4), (2.5) and (2.6). The accommodation coefficient α_M is usually replaced in many studies by values 0.5, 0.8 and 1.0. In this Thesis, the parameter α_M is chosen to be equal to 1. The results are for 400 angles in [0,π], 800 nodes in radial direction and for 80 discrete magnitudes. The algorithm that is used, is confirmed by the results of the current bibliography. The thermal creep flow problem is solved using X_P= 0 and X_T= 1 while the Poiseuille problem (pressure driven flow) is solved using X_P= 1 and X_T= 0 based on Rykov's kinetic problem.

For N_2 $(j = 2, \omega_0 = 0.2354, \omega_1 = 0.3049, \kappa = 0.645)$, the preciseness of the algorithms' results, developed for the present Thesis for the problems of the mass and the heat flow, in comparison with [22] and [23] was confirmed. The relative error is less than 1%.

4.2 Non-Dimensional gas flow through tube

Initially, in every method all the parameters needed for each temperature in both methods are defined. As it is seen in the results, the temperature affects the flow mainly in low temperatures. The calculations were carried out for temperatures T = 300 K, 373.15 K, 423.15 K, 573.15 K, 1000 K and 1500 K and for tangential momentum accommodation coefficient α_M = 1.

4.2.1 Method 1: Analysis and results

The Prandtl number is given for the temperatures T=300K, 373.15K, 423.15, 573.15K 1000K and 1500K from Uribe [27]. In Table 4.1 it is shown the value of Prandtl number in terms of temperature.

Table 4.1: Prandtl Number of N_2 in terms of temperature

	Temperature	*Prandtl Number*
T_1	300 K	0.7215
T_2	373.15 K	0.7102
T_3	423.15 K	0.7043
T_4	573.15 K	0.6917
T_5	1000 K	0.6884
T_6	1500 K	0.6886

Furthermore, the value of parameter Z_{rot} is obtained by eq. (4.1)

$$\mathrm{Z_{rot}} = \frac{\mathrm{Z_{rot}^{\infty}}}{1+\left(\pi^{\frac{1}{2}}\right)\left(\frac{\mathrm{T^*}}{\mathrm{T_{tr}}}\right)^{\frac{1}{2}}+\left(\pi+\frac{\pi^2}{4}\right)\left(\frac{\mathrm{T^*}}{\mathrm{T_{tr}}}\right)} \tag{4.1}$$

where $\mathrm{T_{tr}}$ is the temperature of gas and the parameters $\mathrm{Z_{rot}^{\infty}}$ and T^* are determined by Lordi and Mates model as Z_{rot}^{∞} = 23.0 and T^* = 91.5.

The rotational collision number $Z^{(R)}$ is specified using the equation (4.2):

$$Z^{(R)} = \frac{3\pi}{4(d+3)} Z_{rot} \tag{4.2}$$

where d = 2 the rotational degrees of freedom j.

Both eqs. (4.1) and (4.2) are solved for all temperatures. The Table 4.2 contains all the results of solving eqs. (4.1) and (4.2).

Table 4.2: Rotational collision number $Z^{(R)}$ and Z_{rot} in terms of temperature

	Temperatures	Prandtl Number	Z_{rot}	$Z^{(R)}$
T_1	300 K	0.7215	7.1871	3.3868
T_2	373.15 K	0.7102	8.1728	3.8513
T_3	423.15 K	0.7043	8.7620	4.1290
T_4	573.15 K	0.6917	10.2243	4.8181
T_5	1000 K	0.6884	12.9119	6.0846
T_6	1500 K	0.6886	14.7339	6.9432

In order for the parameters ω_0 and ω_1 to be specified, in the first method the eqs. (2.4) and (2.6) are used. The equation (2.4) is solved for ω_0 where the parameter of power intermolecular potential is κ = 1/1.2. In eq. (2.6), the value of Prandtl number, parameters ω_1 and $Z^{(R)}$ are replaced as given from Table 4.2. The eq. (2.6) is solved in order to specify the parameter ω_1.

Table 4.3: Parameters ω_0 and ω_1 in terms of temperature

	Temperatures	Prandtl	Z_{rot}	$Z^{(R)}$	$\boldsymbol{\omega_0}$	$\boldsymbol{\omega_1}$
T_1	300 K	0.7215	7.1871	3.3868	0.4368	3.3030
T_2	373.15 K	0.7102	8.1728	3.8513	0.4424	4.1124
T_3	423.15 K	0.7043	8.7620	4.1290	0.4451	4.6253
T_4	573.15 K	0.6917	10.2243	4.8181	0.4503	5.9756
T_5	1000 K	0.6884	12.9119	6.0846	0.4568	6.9949
T_6	1500 K	0.6886	14.7339	6.9432	0.4598	7.4380

The numerical results of dimensionless mass flow rate (X_P = 1, X_T = 0) and the dimensionless heat flow rate (X_P = 0, X_T = 1) are calculated for many values of the rarefaction parameter δ_0. It is noticed that in pressure driven flow, the heat flow rate is always 0, $E_{rot,P}$ = 0. The results of W_P, E_P, W_T, $E_{tr,\mathrm{T}}$ and $E_{rot,T}$ are given in Tables 4.4 to 4.7.

Table 4.4: Dimensionless mass flow due to pressure, W_P, in terms of rarefaction parameter δ_0 and temperature

	δ_0	*300K*	*373.15 K*	*423.15K*	*573.15 K*	*1000K*	*1500K*
W_p	*0.01*	1.4769	1.4769	1.4769	1.4769	1.4770	1.4770
	0.1	1.4081	1.4083	1.4083	1.4084	1.4085	1.4086
	0.5	1.3995	1.3983	1.3984	1.3987	1.3991	1.3993
	0.55	1.4035	1.4039	1.4040	1.4044	1.4048	1.4050
	0.60	1.4097	1.4101	1.4102	1.4106	1.4110	1.4112
	0.65	1.4164	1.4168	1.4170	1.4173	1.4176	1.4180
	0.70	1.4235	1.4239	1.4241	1.4245	1.4249	1.4252
	0.75	1.4311	1.4315	1.4316	1.4320	1.4325	1.4327
	1	1.4729	1.4733	1.4735	1.4740	1.4745	1.4747
	1.5	1.5690	1.5695	1.5697	1.5702	1.5708	1.5711
	2	1.6737	1.6742	1.6744	1.6749	1.6756	1.6759
	5	2.3616	2.3621	2.3623	2.3628	2.3633	2.3636
	10	3.5735	3.5738	3.5740	3.5743	3.5747	3.5749
	20	6.0481	6.0483	6.0484	6.0486	6.0489	6.0489
	50	13.5305	13.5306	13.5306	13.5308	13.5309	13.5310

The results, in Table 4.4, of dimensionless mass flow due to pressure in a circular long tube are based on the first method. The value of W_P is increasing in terms of the rarefaction parameter δ_0. For δ_0 between 0.01 and 1, the value of W_P is decreasing and after a specific point is increasing again. At this point, the value of W_P is the lowest and is known in literature as Knudsen Minimum. In terms of temperature, the value of W_P is about stable because the results are dimensionless.

Table 4.5: Dimensionless heat flow due to pressure, E_P, in terms of rarefaction parameter δ_0 and temperature

	δ_0	*300K*	*373.15 K*	*423.15K*	*573.15 K*	*1000K*	*1500K*
E_p	*0.01*	0.7205	0.7206	0.7206	0.7207	0.7207	0.7208
	0.1	0.6169	0.6174	0.6176	0.6181	0.6187	0.6190
	0.5	0.4670	0.4685	0.4692	0.4705	0.4722	0.4730
	0.55	0.4560	0.4575	0.4583	0.4597	0.4615	0.4623
	0.60	0.4458	0.4474	0.4481	0.4496	0.4515	0.4521
	0.65	0.4362	0.4378	0.4386	0.4401	0.4421	0.4430
	0.70	0.4272	0.4289	0.4297	0.4313	0.4332	0.4342
	0.75	0.4187	0.4204	0.4212	0.4229	0.4249	0.4258
	1	0.3819	0.3838	0.3847	0.3865	0.3887	0.3897
	1.5	0.3271	0.3291	0.3300	0.3319	0.3343	0.3354
	2	0.2868	0.2888	0.2897	0.2916	0.2940	0.2951
	5	0.1642	0.1657	0.1664	0.1678	0.1696	0.1704
	10	0.0944	0.0953	0.0958	0.0967	0.0978	0.0983
	20	0.0574	0.0511	0.0513	0.0518	0.0525	0.0528
	50	0.0210	0.0213	0.0214	0.0216	0.0218	0.0220

The results of dimensionless heat flow due to pressure in a circular long tube on the Table 4.5 are based on the first method. The value of E_P is decreasing in terms of the rarefaction parameter δ_0. In terms of temperature, the value of E_P is about stable because the results are dimensionless.

Table 4.6: Dimensionless mass flow due to temperature, W_T, in terms of rarefaction parameter δ_0 and temperature

	δ_0	*300K*	*373.15 K*	*423.15K*	*573.15 K*	*1000K*	*1500K*
W_T	*0.01*	0.7205	0.7206	0.7206	0.7207	0.7207	0.7208
	0.1	0.6169	0.6174	0.6176	0.6181	0.6187	0.6190
	0.5	0.4670	0.4685	0.4692	0.4705	0.4722	0.4730
	0.55	0.45660	0.4575	0.4583	0.4597	0.4615	0.4623
	0.60	0.4458	0.4474	0.4481	0.4496	0.4515	0.4523
	0.65	0.4362	0.4378	0.4386	0.4402	0.4421	0.4430
	0.70	0.4272	0.4289	0.4297	0.4313	0.4332	0.4342
	0.75	0.4187	0.4204	0.4212	0.4229	0.4249	0.4258
	1	0.3819	0.3838	0.3847	0.3865	0.3887	0.3897
	1.5	0.3271	0.3291	0.3300	0.3319	0.3343	0.3354
	2	0.2868	0.2888	0.2897	0.2916	0.2940	0.2951
	5	0.1642	0.1657	0.1664	0.1678	0.1696	0.1704
	10	0.0944	0.0953	0.0958	0.0967	0.0978	0.0983
	20	0.0506	0.0511	0.0513	0.0518	0.0525	0.0528
	50	0.0211	0.0213	0.0214	0.0216	0.0219	0.0220

In Table 4.6 the results of dimensionless mass flow due to temperature in a circular long based on the first method are presented. The value of W_T is decreasing in terms of the rarefaction parameter δ_0. In terms of temperature, the value of W_T is about stable because the results are dimensionless. According to Onsager's relation [21], in the Poiseuille problem, the mass flow rate due to temperature is equal to heat flow due to pressure, which is confirmed comparing the results from Table 4.5 and 4.6.

Table 4.7: Dimensionless heat flow related to translational degrees of freedom due to temperature in terms of rarefaction parameter δ_0 and temperature $E_{tr,T}$ and dimensionless heat flow related to translational degrees of freedom due to temperature in terms of rarefaction parameter δ_0 and temperature, $E_{rot,T}$

δ_0	*300K*		*373.15 K*		*423.15K*	
	$E_{tr,T}$	$E_{rot,T}$	$E_{tr,T}$	$E_{rot,T}$	$E_{tr,T}$	$E_{rot,T}$
0.01	3.2824	1.4606	3.2829	1.4613	3.2832	1.4618
0.1	2.8615	1.2730	2.8650	1.2784	2.8673	1.2827
0.5	2.0853	0.9164	2.0918	0.9257	2.0949	0.9309
0.55	2.0242	0.8881	2.0309	0.8978	2.0341	0.9031
0.60	1.9671	0.8618	1.9740	0.8716	1.9773	0.8771
0.65	1.9136	0.8371	1.9206	0.8472	1.9240	0.8528
0.70	1.8633	0.8138	1.8705	0.8241	1.8739	0.8299
0.75	1.8158	07919	1.8231	0.8024	1.8267	0.8082
1	1.6129	0.6986	1.6244	0.7156	1.6318	0.7294
1.5	1.3212	0.5656	1.3291	0.5764	1.3329	0.5824
2	1.1190	0.4746	1.1261	0.4847	1.1302	0.4904
5	0.5779	0.2382	0.5852	0.2482	0.5900	0.2566
10	0.3167	0.1288	0.3211	0.1346	0.3240	0.1395
20	0.1658	0.0707	0.1673	0.0689	0.1681	0.0700
50	0.0681	0.0290	0.0687	0.0283	0.0691	0.0287

Table 4.7: Continue

δ_0	*573.15 K*		*1000K*		*1500K*	
	$E_{tr,T}$	$E_{rot,T}$	$E_{tr,T}$	$E_{rot,T}$	$E_{tr,T}$	$E_{rot,T}$
0.01	3.2827	1.4610	3.2835	1.4617	3.2837	1.4615
0.1	2.8638	1.2765	2.8700	1.2814	2.8713	1.2798
0.5	2.1010	0.9425	2.1085	0.9389	2.1120	0.9345
0.55	2.0404	0.9151	2.0482	0.9114	2.0519	0.9069
0.60	1.9838	0.8895	1.9919	0.8857	1.9956	0.8810
0.65	1.9308	0.8655	1.9390	0.8615	1.9429	0.8568
0.70	1.8808	0.8428	1.8893	0.8388	1.8932	0.8339
0.75	1.8337	0.8214	1.8423	0.8173	1.8463	0.8124
1	1.6206	0.7095	1.6409	0.7251	1.6451	0.7199
1.5	1.3403	0.5962	1.3496	0.5920	1.3539	0.5868
2	1.1373	0.5035	1.1462	0.4994	1.1504	0.4945
5	0.5828	0.2445	0.5960	0.2539	0.5988	0.2508
10	0.3197	0.1325	0.3275	0.1380	0.3292	0.1361
20	0.1696	0.0727	0.1716	0.0718	0.1725	0.0798
50	0.0697	0.0298	0.0705	0.0294	0.0709	0.0290

On the Table 4.7, the results of dimensionless heat flow related to translational degrees of freedom due to temperature in terms of rarefaction parameter δ_0 and temperature $E_{tr,\mathrm{T}}$ and dimensionless heat flow related to translational degrees of freedom due to temperature in terms of rarefaction parameter δ_0 and temperature, $E_{rot,T}$ in a circular long based on the first method are presented. The value of both $E_{tr,\mathrm{T}}$ and $E_{rot,T}$ is decreasing in terms of the rarefaction parameter δ_0. In terms of temperature, the value of $E_{tr,\mathrm{T}}$ and $E_{rot,T}$ is about stable with ascending tendency because the results are dimensionless.

4.2.2 Method 2: Analysis and results

In contrast with the first method, eqs. (2.4) and (2.5) are used in order to determine the values of ω_0 and ω_1 while the value of Prandtl number is defined from eq. 2.6 as a result of the value of the parameters ω_0 and ω_1.

The parameters ω_0, Z_{rot} and $Z^{(R)}$ have the same values as were calculated in paragraph 4.2.1 and are shown in Table 4.3.

In Table 4.8 the results of system of eqs. (2.5) and (2.6) for ω_1 and Prandtl number respectively are given.

Table 4.8: Parameters Z_{rot}, $Z^{(R)}$, Prandtl Number, ω_0 and ω_1 in terms of temperature

	Temperature	Z_{rot}	$Z^{(R)}$	$\boldsymbol{\omega_0}$	$\boldsymbol{\omega_1}$	*Prandtl*
T_1	300 K	7.1871	3.3868	0.4367	2.7486	0.7291
T_2	373.15 K	8.1727	3.8513	0.4424	2.7707	0.7264
T_3	423.15 K	8.7620	4.1290	0.4451	2.7817	0.7251
T_4	573.15 K	10.2243	4.8181	0.4503	2.8040	0.7224
T_5	1000 K	12.9119	6.0846	0.4568	2.8325	0.7192
T_6	1500 K	14.7339	6.9432	0.4598	2.8463	0.7177

In Tables 4.9 to 4.12, the results of dimensionless mass flow due to temperature W_P, dimensionless heat flow due to pressure E_P, dimensionless mass flow due to temperature W_T, dimensionless heat flow related to translational degrees of freedom due to temperature in terms of rarefaction parameter δ_0 and temperature $E_{tr,\mathrm{T}}$ and dimensionless heat flow related to translational degrees of freedom due to temperature in terms of rarefaction parameter δ_0 and temperature, $E_{rot,T}$ in a circular long tube based on the second method are presented.

Table 4.9: Dimensionless mass flow due to pressure, , W_P, in terms of rarefaction parameter δ_0 and temperature.

	δ_0	*300K*	*373.15 K*	*423.15K*	*573.15 K*	*1000K*	*1500K*
W_p	*0.01*	1.4769	1.4769	1.4769	1.4769	1.4769	1.4770
	0.1	1.4081	1.4083	1.4083	1.4084	1.4085	1.4086
	0.5	1.3980	1.3983	1.3984	1.3987	1.3991	1.3993
	0.55	1.4035	1.4039	1.4040	1.4044	1.4048	1.4050
	0.60	1.4097	1.4101	1.4102	1.4106	1.4110	1.4112
	0.65	1.4164	1.4168	1.4170	1.4173	1.4178	1.4180
	0.70	1.4235	1.4239	1.4241	1.4245	1.4249	1.4252
	0.75	1.4311	1.4315	1.4316	1.4320	1.4325	1.4327
	1	1.4729	1.4733	1.4735	1.4740	1.4745	1.4748
	1.5	1.5690	1.5695	1.5697	1.5702	1.5708	1.5711
	2	1.6737	1.6742	1.6744	1.6749	1.6756	1.6759
	5	2.3616	2.3621	2.3623	2.3628	2.3633	2.3636
	10	3.5735	3.5738	3.5740	3.5743	3.5747	3.5749
	20	6.0481	6.0483	6.0484	6.0486	6.0489	6.0490
	50	13.5305	13.5306	13.5307	13.5308	13.5309	13.5310

Table 4.10: Dimensionless heat flow due to pressure, E_P, in terms of rarefaction parameter δ_0 and temperature

	δ_0	300K	373.15 K	423.15K	573.15 K	1000K	1500K
E_P	0.01	0.7205	0.7206	0.7206	0.7207	0.7207	0.7208
	0.1	0.6169	0.6174	0.6176	0.6181	0.6187	0.6190
	0.5	0.4670	0.4685	0.4692	0.4705	0.4722	0.4730
	0.55	0.4560	0.4575	0.4583	0.4597	0.4615	0.4623
	0.60	0.4458	0.4474	0.4481	0.4496	0.4515	0.4523
	0.65	0.4362	0.4378	0.4386	0.4402	0.4421	0.4430
	0.70	0.4272	0.4289	0.4297	0.4313	0.4332	0.4342
	0.75	0.4187	0.4204	0.4212	0.4229	0.4289	0.4258
	1	0.3819	0.3838	0.3847	0.3865	0.3887	0.3897
	1.5	0.3271	0.3291	0.3300	0.3319	0.3343	0.3354
	2	0.2868	0.2888	0.2897	0.2916	0.2940	0.2951
	5	0.1642	0.1657	0.1664	0.1678	0.1696	0.1704
	10	0.0944	0.0953	0.0958	0.0967	0.0978	0.0 983
	20	0.0506	0.0511	0.0513	0.0518	0.0525	0.0528
	50	0.0210	0.0213	0.0214	0.0216	0.0219	0.0220

Table 4.11: Dimensionless mass flow due to temperature, W_T, in terms of rarefaction parameter δ_0 and temperature

	δ_0	*300K*	*373.15 K*	*423.15K*	*573.15 K*	*1000K*	*1500K*
W_T	*0.01*	0.7205	0.7206	0.7206	0.7207	0.7207	0.7208
	0.1	0.6169	0.6174	0.6176	0.6181	0.6187	0.6190
	0.5	0.4670	0.4685	0.4692	0.4705	0.4722	0.4730
	0.55	0.4560	0.4575	0.4583	0.4597	0.4615	0.4623
	0.60	0.4458	0.4474	0.4481	0.4496	0.4515	0.4523
	0.65	0.4362	0.4378	0.4386	0.4402	0.4421	0.4430
	0.70	0.4272	0.4289	0.4297	0.4313	0.4332	0.4342
	0.75	0.4187	0.4204	0.4212	0.4229	0.4249	0.4258
	1	0.3819	0.3838	0.3847	0.3865	0.3887	0.3897
	1.5	0.3271	0.3291	0.3300	0.3319	0.3343	0.3354
	2	0.2868	0.2888	0.2897	0.2916	0.2940	0.2951
	5	0.1642	0.1657	0.1664	0.1678	0.1696	0.1704
	10	0.0944	0.0953	0.0958	0.0967	0.0978	0.0983
	20	0.0506	0.0511	0.0513	0.0518	0.0525	0.0528
	50	0.0210	0.0213	0.0214	0.0216	0.0219	0.0220

Table 4.12: Dimensionless heat flow related to translational degrees of freedom due to temperature in terms of rarefaction parameter δ_0 and temperature $E_{tr,T}$ and dimensionless heat flow related to translational degrees of freedom due to temperature in terms of rarefaction parameter δ_0 and temperature, $E_{rot,T}$

δ_0	*300 K*		*373.15 K*		*423.15 K*	
	$E_{rot,T}$	$E_{tr,T}$	$E_{rot,T}$	$E_{tr,T}$	$E_{rot,T}$	$E_{tr,T}$
0.01	3.2824	1.4500	3.2827	1.4598	3.2829	1.4597
0.1	2.8615	1.2685	2.8638	1.2670	2.8650	1.2662
0.5	2.0854	0.9048	2.0918	0.9009	2.0949	0.8990
0.55	2.0242	0.8762	2.0309	0.8721	2.0341	0.8701
0.60	1.9671	0.8495	1.9740	0.8453	1.9772	0.8433
0.65	1.9136	0.8245	1.9206	0.8202	1.9240	0.8181
0.70	1.8633	0.8011	1.8705	0.7967	1.8739	0.7946
0.75	1.8158	0.7790	1.8231	0.7746	1.8267	0.7724
1	1.6129	0.6852	1.6206	0.6807	1.6244	0.6784
1.5	1.3213	0.5525	1.3291	0.5481	1.3329	0.5459
2	1.1191	0.4623	1.1265	0.4582	1.1302	0.4561
5	0.5779	0.2306	0.5828	0.2280	0.5852	0.2268
10	0.3167	0.1244	0.3197	0.1229	0.3211	0.1222
20	0.1657	0.0645	0.1673	0.0637	0.1681	0.0634
50	0.0680	0.0264	0.0687	0.0261	0.0691	0.0259

Table 4.12: Continue

δ_0	*573.15 K*		*1000K*		*1500K*	
	$E_{rot,T}$	$E_{tr,T}$	$E_{rot,T}$	$E_{tr,T}$	$E_{rot,T}$	$E_{tr,T}$
0.01	3.2832	1.4595	3.2835	1.4592	3.2837	1.4591
0.1	2.8673	1.2646	2.8700	1.2626	2.8713	1.2617
0.5	2.1010	0.8950	2.1085	0.8900	2.1120	0.8877
0.55	2.0404	0.8661	2.0482	0.8609	2.0519	0.8585
0.60	1.9838	0.8391	1.9919	0.8339	1.9956	0.8313
0.65	1.9307	0.8139	1.9390	0.8086	1.9429	0.8060
0.70	1.8808	0.7903	1.8893	0.7849	1.8932	0.7823
0.75	1.8337	0.7681	1.8423	0.7626	1.8463	0.7600
1	1.6318	0.6740	1.6409	0.6683	1.6451	0.6656
1.5	1.3403	0.5416	1.3496	0.5361	1.3539	0.5335
2	1.1373	0.4521	1.1462	0.4471	1.1504	0.4446
5	0.5900	0.2243	0.5960	0.2212	0.5988	0.2197
10	0.3240	0.1208	0.3275	0.1190	0.3292	0.1182
20	0.1696	0.0626	0.1716	0.0616	0.1725	0.0612
50	0.0697	0.0256	0.0705	0.0252	0.0709	0.0250

The results of Tables 4.9 to 4.12 (Method 1) are similar with the results of Tables 4.4 to 4.7 (Method 2).

4.3 Comparison of the two methods

It is significant to compare the Prandtl number that was used in both cases. In the first method, the Prandtl number is stated in any temperature from [27]. In the second method, the system of equations that were described analytically is needed to be solved. Prandtl number is a dimensionless parameter and depends on the fluid properties. There are many equations that can be used in order to specify its value. Also, its value can be defined by experimental studies. In the Table 4.13, the value of Prandtl number from Table 4.1, Table 4.7 and EES program [28] is compared.

Table 4.13: Comparison of Prandtl Number of the two methods in terms of temperature

	Temperature	*Prandtl [18] (Method 1)*	*Prandtl Table 4.5 (Method 2)*	*Prandtl [19]*
T_1	300 K	0.7215	0.7291	0.7134
T_2	373.15 K	0.7102	0.7264	0.7056
T_3	423.15 K	0.7043	0.7250	0.7025
T_4	573.15 K	0.6917	0.7224	0.7078
T_5	1000 K	0.6884	0.7192	0.7243
T_6	1500 K	0.6886	0.7177	0.6632

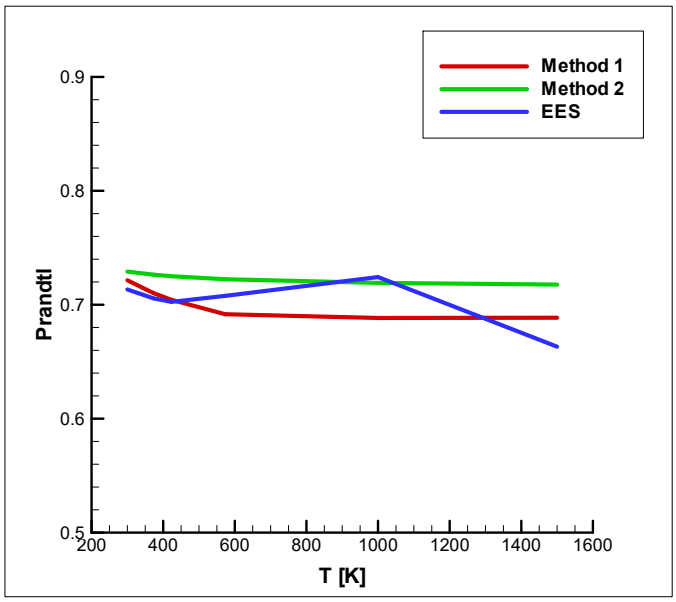

Figure 4.1: Value of Prandtl Number of the two methods in terms of temperature

The value of parameter ω_0 is the same in Method 1 and Method 2. In the first method, the eq. (2.6) in order to specify the parameter ω_1 was used, while in the second method the eq. (2.5) was used. As it is seen, the growth rate of parameter ω_1 is bigger in the first method than it is in the second. In Table 4.14 and Figure 4.2, the value of ω_1 is compared.

Table 4.14: Comparison of value of parameter ω_1 of the two methods in terms of temperature

	Temperature	ω_1 *(Method 1)*	ω_1 *(Method 2)*
T_1	*300 K*	3.3030	2.7486
T_2	*373.15 K*	4.1124	2.7707
T_3	*423.15 K*	4.6253	2.7817
T_4	*573.15 K*	5.9756	2.8040
T_5	*1000 K*	6.9949	2.8325
T_6	*1500 K*	7.4380	2.8463

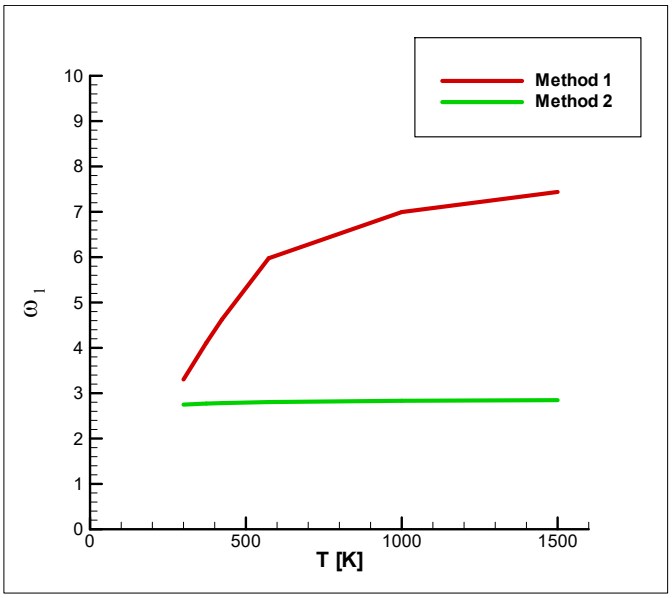

Figure 4.2: Value of Parameter ω_1 of the two methods in terms of temperature

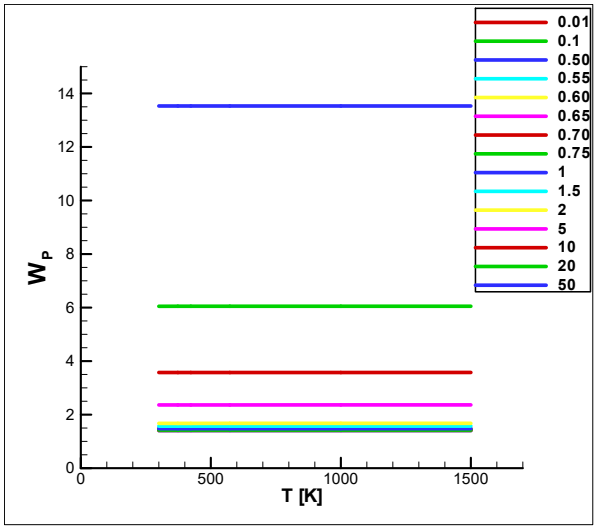

Figure 4.3: Value of dimensionless mass flow due to pressure, W_P, in terms of rarefaction parameter δ_0 and temperature

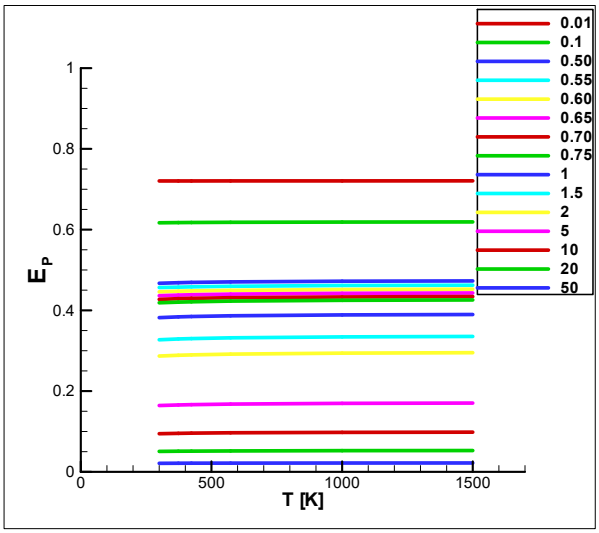

Figure 4.4: Value of dimensionless heat flow due to pressure, E_P, in terms of rarefaction parameter δ_0 and temperature

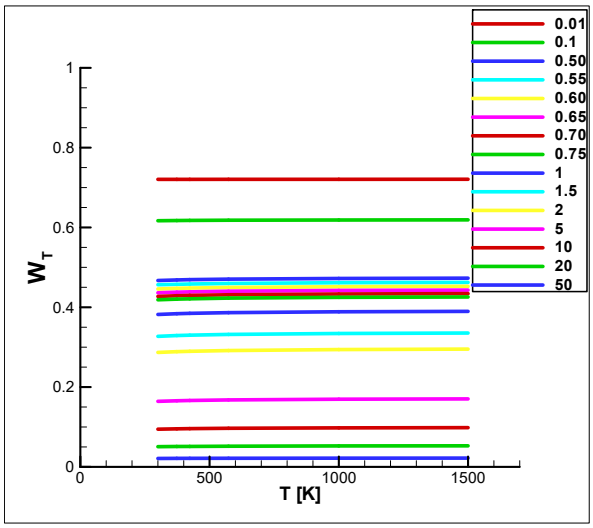

Figure 4.5: Value of dimensionless mass flow due to temperature, W_T, in terms of rarefaction parameter δ_0 and temperature

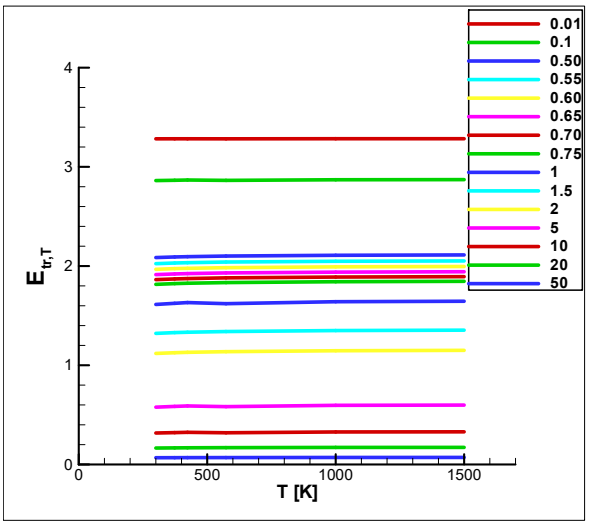

Figure 4.6: Dimensionless heat flow related to translational degrees of freedom due to temperature, $E_{tr,T}$, in terms of rarefaction parameter δ_0 and temperature

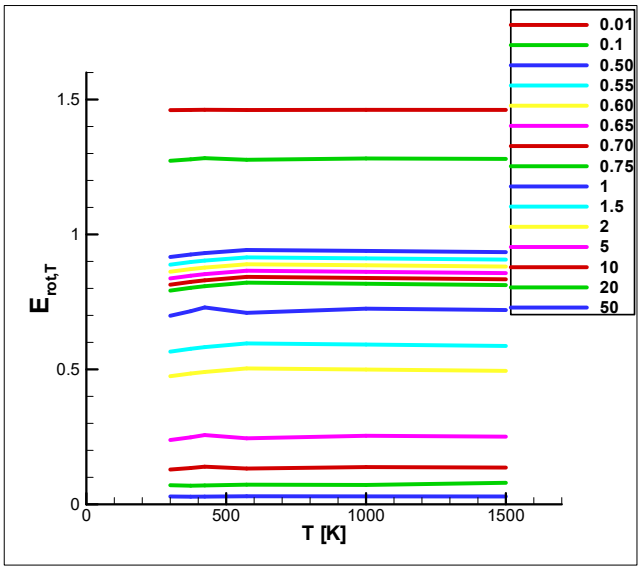

Figure 4.7: Dimensionless heat flow related to rotational degrees of freedom due to temperature $E_{rot,T}$ in terms of rarefaction parameter δ_0 and temperature

It is needed to be remarked that in Figure 4.7, there seems to be an ubnormal behavior of value of $E_{rot,T}$ especially for $\delta_0 = 1.5 \; and \; \delta_0 = 1$. So, it is obligatory to check the results of the non-dimensional calculations for a dimensional solution in paragraph 4.4.

There are no differences between using the two methods in the determination of W_P, E_P and W_T. The only differences that can be detected are in parameters $E_{tr,T}$ and $E_{rot,T}$. On the Table 4.15, there is a comparison between the value of $E_{tr,T}$ and $E_{rot,T}$ for temperature $T = 423.15\ K$.

Table 4.15: Comparison of $E_{tr,T}$ and $E_{rot,T}$ of the two methods for $T = 423.15K$

δ_0	*423.15K*			
	$E_{tr,T}$ *Method 1*	$E_{tr,T}$ *Method 2*	$E_{rot,T}$ *Method 1*	$E_{rot,T}$ *Method 2*
0.01	3.2832	3.2829	1.4618	1.4597
0.1	2.8673	2.8650	1.2827	1.2662
0.5	2.0949	2.0949	0.9309	0.8990
0.55	2.0341	2.0341	0.9031	0.8701
0.60	1.9773	1.9772	0.8771	0.8433
0.65	1.9240	1.9240	0.8528	0.8181
0.70	1.8739	1.8739	0.8299	0.7946
0.75	1.8267	1.8267	0.8082	0.7724
1	1.6318	1.6244	0.7294	0.6784
1.5	1.3329	1.3329	0.5824	0.5459
2	1.1302	1.1302	0.4904	0.4561
5	0.5900	0.5852	0.2566	0.2268
10	0.3240	0.3211	0.1395	0.1222
20	0.1681	0.1681	0.0700	0.0634
50	0.0691	0.0691	0.0287	0.0259

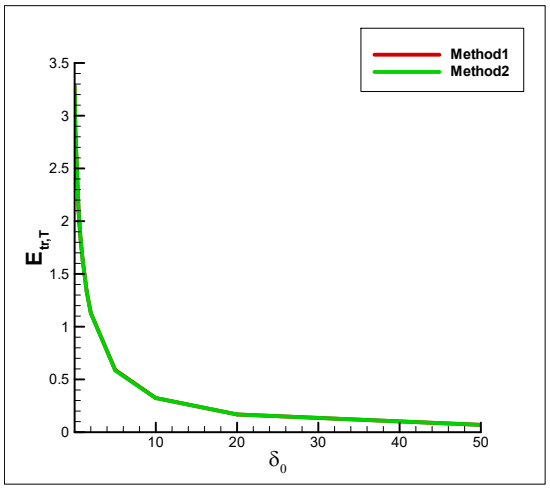

Figure 4.8: Comparison of $E_{tr,T}$ of the two methods

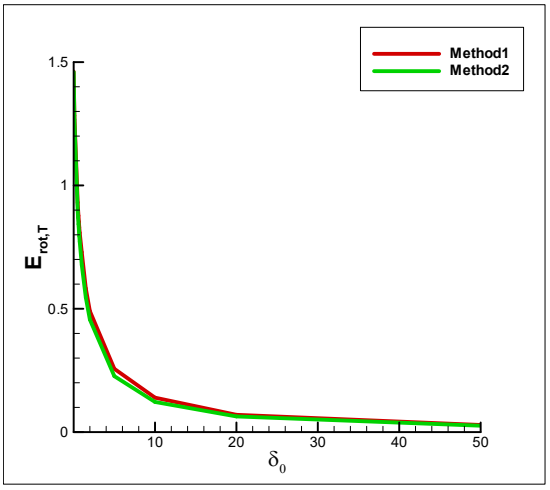

Figure 4.9: Comparison of $E_{rot,T}$ of the two methods

It should be mentioned that the value of $E_{tr,\mathrm{T}}$ is almost the same in both methods. In contrast, the value of $E_{rot,T}$ is not the same. The calculation of dimensionless heat flow related to rotational degrees of freedom due to temperature depends on the value of the parameter ω_1 while the calculation of dimensionless heat flow related to translational degrees of freedom due to temperature depends on the value of ω_0. In both methods, the value of the parameter ω_0 is the same and as a result the value of heat flow due to translational degrees of freedom. The different value of the parameter ω_1 results to different values for $E_{rot,T}$.

4.4 Dimensional gas flow through tube

The experimental results of the mass flow in tubes are dimensional. The databases that were presented in paragraphs 4.2.1 and 4.2.2 are dimensionless, so they can be used for many cases. They are needed to be dimensionalized using the parameters of the experimental research in order to be compared. Because in paragraphs 4.2 and 4.3 the results of both methods were the same, all the calculations are conducted in order to verify that the results are valid based on the dimensionless results of Method 1.

In Figures 4.3, 4.4, 4.5, 4.6 and 4.7 the dimensionless results of Method 1 are presented, which are the same as method 2. The value of the dimensionless parameters in terms of temperature are almost stable. In order for the dimensionless results to be verified, they are required to be dimensional.

The dimensionless results are converted to dimensional through eq. (4.3), where the parameters are assigned dimensional values.

$$\delta_0 = \frac{P_0 R_{RAD}}{\mu_0 u_0} \Rightarrow \quad \delta_0 \mu_0 u_0 = P_0 R_{RAD} \Rightarrow \quad P_0 = \delta_0 \mu_0 u_0 / R_{RAD} \Rightarrow$$

$$\Rightarrow \quad P_0 u_0 = \delta_0 \mu_0 u_0^2 \ / R_{RAD} \ , \ \{\text{where} \quad R_{RAD} = D\} \Rightarrow$$

$$\Rightarrow \quad P_0 u_0 = \delta_0 \mu_0 u_0^2 \ / D \ , \{\text{with } u_0 = \sqrt{2RT_0}^2 = 2RT_0\} \Rightarrow$$

$$\Rightarrow \quad P_0 u_0 = \delta_0 \mu_0 2RT_0 / D \quad (4.3)$$

with radius $D = 5 * 10^{-3} \{m\}$

parameter $\delta_0 = 0.5$,

dimensionless pressure P_0, dimensionless velocity u_0,

constant of N_2 $R = 296.80 \{J/(Kg\ K)\}$, viscosity μ_0

In Table 4.16 the viscosity of N_2 is given by [28] the results of solving the eq. 4.3 for $\mathrm{P}_0\mathrm{u}_0$ for the temperatures $T = 300\,K, 373.15\,K, 423.15\,K, 573.15\,K, 1000\,K$ and $1500\,K$ are presented below.

Table 4.16: Viscosity and $\mathrm{P}_0\mathrm{u}_0$ in terms of temperature

Temperature (T_0) {K}	*Viscosity* (μ_0) $\{Kg/m*s\}$	$\boldsymbol{P_0 u_0}$
300	0.00001768	314.8454
373.15	0.00002094	463.8249
423.15	0.000023	577.7182
573.15	0.00002849	969.2920
1000	0.00004013	2382.1168
1500	0.0000504	4487.6160

As it is already mentioned, the values of W_P, E_P, W_T, $E_{tr,T}$ and $E_{rot,T}$ in both methods, have no differences. The results were converted to dimensional for the chosen value of the rarefaction parameter $\delta_0 = 0.5$.

- *Dimensional mass flow due to pressure W_P in terms of temperature*

Table 4.17: Dimensional mass flow due to pressure W_P in terms of temperature

Temperature (T_0) {K}	W_P	$W_P P_0 u_0$
300	1.3980	440.1539
373.15	1.3983	648.5662
423.15	1.3984	807.8812
573.15	1.3987	1355.7488
1000	1.3991	3332.8196
1500	1.3993	6279.5211

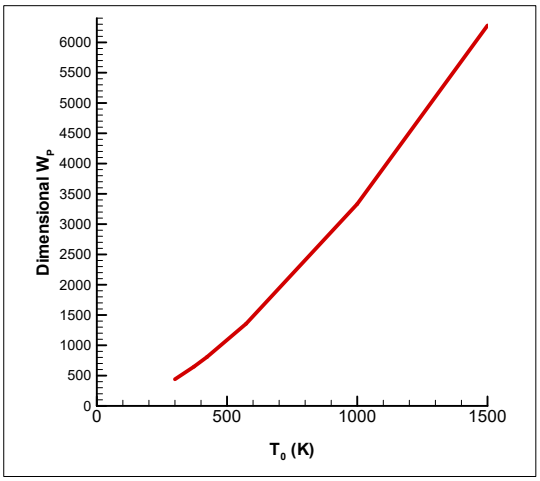

Figure 4.10: Dimensional mass flow due to pressure W_P in terms of temperature

- *Dimensional heat flow due to pressure E_P in terms of temperature*

Table 4.18: Dimensional heat flow due to pressure E_P in terms of temperature

Temperature (T_0) {K}	E_P	$E_P P_0 u_0$
300	0.4670	147.0328
373.15	0.4685	217.3019
423.15	0.4692	271.0654
573.15	0.4705	456.0519
1000	0.4722	1124.8356
1500	0.4730	2122.6424

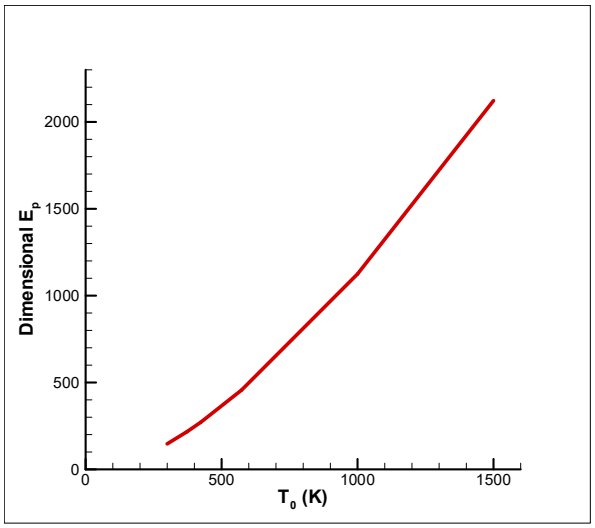

Figure 4.11: Dimensional mass flow due to pressure E_P in terms of temperature

- *Dimensional mass flow due to temperature W_T in terms of temperature*

Table 4.19: Dimensional heat flow due to pressure W_T in terms of temperature.

Temperature (T_0) {K}	W_T	$W_T P_0 u_0$
300	0.4670	147.0328
373.15	0.4685	217.3019
423.15	0.4692	271.0654
573.15	0.4705	456.0519
1000	0.4722	1124.8356
1500	0.4730	2122.6424

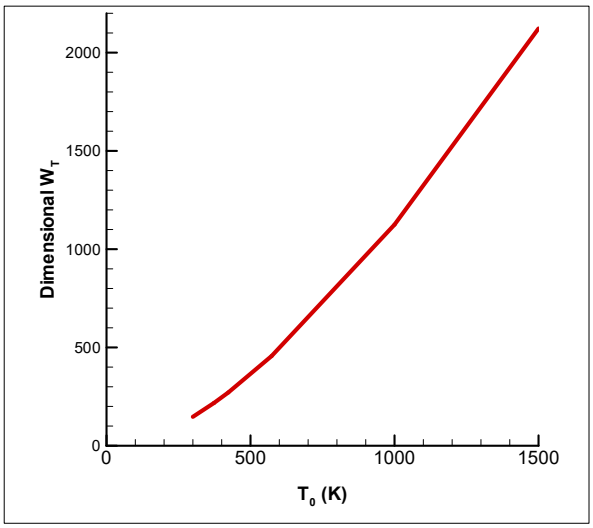

Figure 4.12: Dimensional mass flow due to temperature W_T in terms of temperature.

- *Dimensional heat flow related to translational degrees of freedom due to temperature $E_{tr,T}$ in terms of temperature*

Table 4.20: Dimensional heat flow related to translational degrees of freedom due to temperature $E_{tr,T}$ in terms of temperature

Temperature (T_0) {K}	$E_{tr,T}$	$E_{tr,T}P_0u_0$
300	2.0853	656.5472
373.15	2.0918	970.2288
423.15	2.0949	1210.2619
573.15	2.1010	2036.4825
1000	2.2085	5022.6933
1500	2.1120	9477.8450

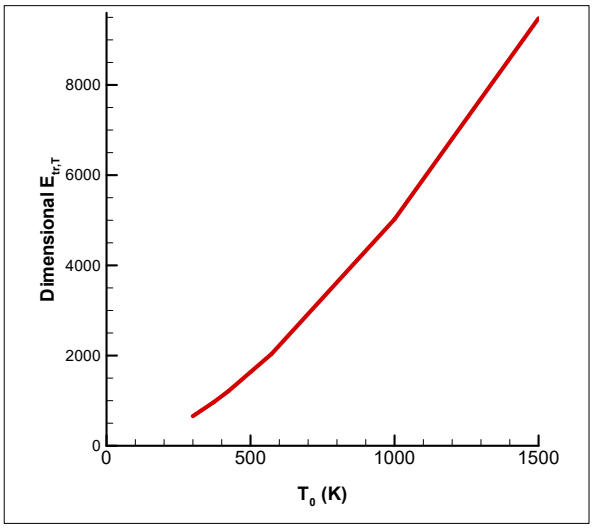

Figure 4.13: Dimensional heat flow related to translational degrees of freedom due to temperature $E_{tr,T}$ in terms of temperature

- *Dimensional heat flow related to rotational degrees of freedom due to temperature $E_{rot,T}$ in terms of temperature*

Table 4.21: Dimensional heat flow related to rotational degrees of freedom due to temperature $E_{rot,T}$ in terms of temperature

Temperature (T_0) {K}	$E_{rot,T}$	$E_{rot,T}P_0u_0$
300	0.9164	288.5243
373.15	0.9257	429.3627
423.15	0.9309	537.7979
573.15	0.9425	913.5577
1000	0.9389	2236.5695
1500	0.9345	4193.6772

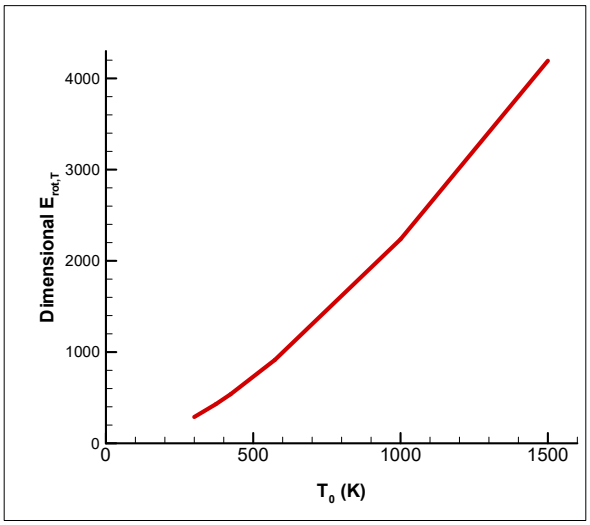

Figure 4.14: Dimensional heat flow related to rotational degrees of freedom due to temperature $E_{rot,T}$ in terms of temperature

All the functions of Figures 4.10 to 4.14 are monotonically increasing, which proves the validity of the dimensionless results. In paragraph 5.1, the dimensionless results of paragraphs 4.2.1 and 4.2.2 are compared with database from [29].

Chapter 5. FULLY DEVELOPED GAS FLOW THROUGH TAPERED CHANNELS

A tapered channel is a sum of circular cross-sections of different radius. In order to specify the mass and heat flow, the results of Chapter 4 should be compared with validated data from literature. In the literature, there is an extensive research for rarefied monoatomic gas flow in fixed radius tubes and tapered channels, while for polyatomic gases there is limited research for tapered channels, due to its complexity. In the Chapter 5, the flow for monoatomic Nitrogen in tapered channels and for polyatomic Nitrogen in fixed radius tube and tapered channels is investigated.

5.1 Verification of database

In order to validate the results of the databases that were developed in paragraphs 4.2.1 and 4.2.2, the database of the paragraph 4.2.1 is compared with the database of [29], because the results in both databases in paragraphs 4.2.1 and 4.2.2 are the same.

The first comparison is database of 4.2.1 with [29] where the Nitrogen is assumed that it is a monoatomic molecule. In contrast, for the second comparison, the Nitrogen is considered to be a polyatomic molecule.

In [29] the mass flow is presented in terms of the rarefaction parameter δ_0 and ω. Contrariwise, in the databases that were developed in Chapter 4, the mass flow is presented in terms of the rarefaction parameter δ_0 and temperature. The value of ω for monoatomic Nitrogen, is equal to 1. In Table 4.5, the results of mass flow due to pressure and temperature in terms of rarefaction parameter δ_0 from paragraph 4.2.1 and [29] are being compared.

Table 5.1: Comparison of dimensionless mass flow due to pressure in terms of rarefaction parameter δ_0 and temperature for monoatomic Nitrogen

		Database Sub. 4.2.1	*[29]*	*Database Sub. 4.2.1*	*[29]*	*Database Sub. 4.2.1*	*[29]*
	δ_0	*300K*		*373.15 K*		*423.15K*	
W_P	*0.01*	1.4769	1.4770	1.4769	1.4770	1.4769	1.4770
	0.1	1.4081	1.4090	1.4083	1.4090	1.4083	1.4090
	0.5	1.3995	1.4005	1.3983	1.4005	1.3984	1.4005
	0.55	1.4035	1.4062	1.4039	1.4062	1.4040	1.4062
	0.60	1.4097	1.4125	1.4101	1.4125	1.4102	1.4125
	0.65	1.4164	1.4194	1.4168	1.4194	1.4170	1.4194
	0.70	1.4235	1.4266	1.4239	1.4266	1.4241	1.4266
	0.75	1.4311	1.4342	1.4315	1.4342	1.4316	1.4342
	1	1.4729	1.4764	1.4733	1.4764	1.4735	1.4764
	1.5	1.5690	1.5730	1.5695	1.5730	1.5697	1.5730
	2	1.6737	1.6779	1.6742	1.6779	1.6744	1.6779
	5	2.3616	2.3654	2.3621	2.3654	2.3623	2.3654
	10	3.5735	3.5761	3.5738	3.5761	3.5740	3.5761
	20	6.0481	6.0496	6.0483	6.0496	6.0484	6.0496
	50	13.5305	13.531	13.5306	13.531	13.5306	13.531

Table 5.1: Continue

		Database Sub. 4.2.1	*[29]*	*Database Sub. 4.2.1*	*[29]*	*Database Sub. 4.2.1*	*[29]*
	δ_0	*573.15 K*		*1000K*		*1500K*	
W_P	*0.01*	1.4769	1.4770	1.4770	1.4770	1.4770	1.4770
	0.1	1.4084	1.4090	1.4085	1.4090	1.4086	1.4090
	0.5	1.3987	1.4005	1.3991	1.4005	1.3993	1.4005
	0.55	1.4044	1.4062	1.4048	1.4062	1.4050	1.4062
	0.60	1.4106	1.4125	1.4110	1.4125	1.4112	1.4125
	0.65	1.4173	1.4194	1.4176	1.4194	1.4180	1.4194
	0.70	1.4245	1.4266	1.4249	1.4266	1.4252	1.4266
	0.75	1.4320	1.4342	1.4325	1.4342	1.4327	1.4342
	1	1.4740	1.4764	1.4745	1.4764	1.4747	1.4764
	1.5	1.5702	1.5730	1.5708	1.5730	1.5711	1.5730
	2	1.6749	1.6779	1.6756	1.6779	1.6759	1.6779
	5	2.3628	2.3654	2.3633	2.3654	2.3636	2.3654
	10	3.5743	3.5761	3.5747	3.5761	3.5749	3.5761
	20	6.0486	6.0496	6.0489	6.0496	6.0489	6.0496
	50	13.5308	13.531	13.5309	13.531	13.5310	13.531

In Table 5.1, the results of the dimensionless mass flow due to pressure are being compared with [29] from the literature. The differences of the dimensionless mass flow, due to pressure, for a tapered channel between paragraph 4.2.1 and [29] are miniscule.

Table 5.2: Comparison of dimensionless mass flow due to temperature in terms of rarefaction parameter δ_0 and temperature for monoatomic Nitrogen N_2

		Database Sub. 4.2.1	*[29]*	*Database Sub. 4.2.1*	*[29]*	*Database Sub. 4.2.1*	*[29]*
	δ_0	*300K*		*373.15 K*		*423.15K*	
W_T	*0.01*	0.7205	0.7210	0.7206	0.7210	0.7206	0.7210
	0.1	0.6169	0.6209	0.6174	0.6209	0.6176	0.6209
	0.5	0.4670	0.4784	0.4685	0.4784	0.4692	0.4784
	0.55	0.45660	0.4680	0.4575	0.4680	0.4583	0.4680
	0.60	0.4458	0.4582	0.4474	0.4582	0.4481	0.4582
	0.65	0.4362	0.4491	0.4378	0.4491	0.4386	0.4491
	0.70	0.4272	0.4404	0.4289	0.4404	0.4297	0.4404
	0.75	0.4187	0.4323	0.4204	0.4323	0.4212	0.4323
	1	0.3819	0.3967	0.3838	0.3967	0.3847	0.3967
	1.5	0.3271	0.3430	0.3291	0.3430	0.3300	0.3430
	2	0.2868	0.3027	0.2888	0.3027	0.2897	0.3027
	5	0.1642	0.1762	0.1657	0.1762	0.1664	0.1762
	10	0.0944	0.1020	0.0953	0.1020	0.0958	0.1020
	20	0.0506	0.0548	0.0511	0.0548	0.0513	0.0548
	50	0.0211	0.0223	0.0213	0.0223	0.0214	0.0223

Table 5.2: Continue

		Database Sub. 4.2.1	*[29]*	*Database Sub. 4.2.1*	*[29]*	*Database Sub. 4.2.1*	*[29]*
	δ_0	*573.15 K*		*1000K*		*1500K*	
W_T	*0.01*	0.7207	0.7210	0.7207	0.7210	0.7208	0.7210
	0.1	0.6181	0.6209	0.6187	0.6209	0.6190	0.6209
	0.5	0.4705	0.4784	0.4722	0.4784	0.4730	0.4784
	0.55	0.4597	0.4680	0.4615	0.4680	0.4623	0.4680
	0.60	0.4496	0.4582	0.4515	0.4582	0.4523	0.4582
	0.65	0.4402	0.4491	0.4421	0.4491	0.4430	0.4491
	0.70	0.4313	0.4404	0.4332	0.4404	0.4342	0.4404
	0.75	0.4229	0.4323	0.4249	0.4323	0.4258	0.4323
	1	0.3865	0.3967	0.3887	0.3967	0.3897	0.3967
	1.5	0.3319	0.3430	0.3343	0.3430	0.3354	0.3430
	2	0.2916	0.3027	0.2940	0.3027	0.2951	0.3027
	5	0.1678	0.1762	0.1696	0.1762	0.1704	0.1762
	10	0.0967	0.1020	0.0978	0.1020	0.0983	0.1020
	20	0.0518	0.0548	0.0525	0.0548	0.0528	0.0548
	50	0.0216	0.0229	0.0219	0.0229	0.0220	0.0229

In order to compare the database that was introduced in paragraphs 4.2.1 and 4.2.2 with [29], for polyatomic Nitrogen, the eq. (5.1) needs to be used, which connects the parameter ω with ω_0, because the value of ω is not 1 as for monoatomic N_2.

$$\omega = \frac{(Z_{rot} - 1 + \omega_0)}{Z_{rot}} \tag{5.1}$$

In order to solve the eq. 5.1., the parameters Z_{rot} and ω_0 need to be specified. The value of ω_0 is given in Table 4.3 for different temperatures. The value of collision number Z_{rot} can be found from the equation:

$$\frac{Z_{rot}^{\infty}}{Z_{rot}} = 1 + \frac{\pi^{3/2}}{2\sqrt{T^*}} + \left(2 + \frac{\pi^2}{4}\right)\frac{1}{T^*} + \left(\frac{\pi}{T^*}\right)^{3/2} \tag{5.2}$$

where $T^* = {kT_0}/{\varepsilon}$ and the values of Z_{rot}^{∞} and ${\varepsilon}/{k}$ are tabulated from the literature [27].

The mass flow due to pressure and due to temperature in [18] is presented in terms of rarefaction parameter δ_0 and ω. In order to compare the results of paragraph 4.2.1 and [29], the value of the mass flow of [29] is calculated using linear interpolation.

The results for the value of T^*, Zrot and ω are given in Table 5.3.

Table 5.3: $\boldsymbol{T^*}$, Z_{rot} and ω in terms of temperature and $\boldsymbol{\omega_0}$

	Temperatures	$\boldsymbol{\omega_0}$	$\boldsymbol{T^*}$	Z_{rot}	ω
T_1	*300 K*	0.4368	3.0488	5.7776	0.9025
T_2	*373.15 K*	0.4424	3.7922	6.7633	0.9176
T_3	*423.15 K*	0.4451	4.3003	7.3641	0.9246
T_4	*573.15 K*	0.4503	5.8247	8.8944	0.9382
T_5	*1000 K*	0.4568	10.1626	11.8721	0.9542
T_6	*1500 K*	0.4598	15.2439	14.0495	0.9616

Table 5.4: Comparison of dimensionless mass flow due to pressure in terms of rarefaction parameter δ_0 and temperature for polyatomic Nitrogen

		Database Sub. 4.2.1	*[29]*	*Database Sub. 4.2.1*	*[29]*	*Database Sub. 4.2.1*	*[29]*
	δ_0	*300K*		*373.15 K*		*423.15K*	
W_P	*0.01*	1.4769	1.4769	1.4769	1.4769	1.4769	1.4770
	0.1	1.4081	1.4085	1.4083	1.4086	1.4083	1.4086
	0.5	1.3995	1.3990	1.3983	1.3992	1.3984	1.3993
	0.55	1.4035	1.4046	1.4039	1.4049	1.4040	1.4050
	0.60	1.4097	1.4109	1.4101	1.4111	1.4102	1.4112
	0.65	1.4164	1.4176	1.4168	1.4179	1.4170	1.4180
	0.70	1.4235	1.4248	1.4239	1.4251	1.4241	1.4252
	0.75	1.4311	1.4323	1.4315	1.4326	1.4316	1.4327
	1	1.4729	1.4743	1.4733	1.4746	1.4735	1.4747
	1.5	1.5690	1.5706	1.5695	1.5710	1.5697	1.5711
	2	1.6737	1.6753	1.6742	1.6757	1.6744	1.6759
	5	2.3616	2.3631	2.3621	2.3634	2.3623	2.3636
	10	3.5735	3.5745	3.5738	3.5747	3.5740	3.5748
	20	6.0481	6.0485	6.0483	6.0487	6.0484	6.0488
	50	13.5305	13.5303	13.5306	13.5304	13.5306	13.5305

Table 5.4: Continue

		Database Sub. 4.2.1	*[29]*	*Database Sub. 4.2.1*	*[29]*	*Database Sub. 4.2.1*	*[29]*
	δ_0	*573.15K*		*1000K*		*1500K*	
W_P	*0.01*	1.4769	1.4770	1.4770	1.4770	1.4770	1.4770
	0.1	1.4084	1.4087	1.4085	1.4087	1.4086	1.4088
	0.5	1.3987	1.3995	1.3991	1.3998	1.3993	1.3999
	0.55	1.4044	1.4052	1.4048	1.4055	1.4050	1.4056
	0.60	1.4106	1.4115	1.4110	1.4117	1.4112	1.4118
	0.65	1.4173	1.4182	1.4176	1.4185	1.4180	1.4187
	0.70	1.4245	1.4254	1.4249	1.4257	1.4252	1.4259
	0.75	1.4320	1.4330	1.4325	1.4333	1.4327	1.4335
	1	1.4740	1.4751	1.4745	1.4754	1.4747	1.4756
	1.5	1.5702	1.5714	1.5708	1.5719	1.5711	1.5720
	2	1.6749	1.6762	1.6756	1.6767	1.6759	1.6769
	5	2.3628	2.3639	2.3633	2.3643	2.3636	2.3644
	10	3.5743	3.5750	3.5747	3.5753	3.5749	3.5754
	20	6.0486	6.0489	6.0489	6.0490	6.0489	6.0492
	50	13.5308	13.5306	13.5309	13.5306	13.5310	13.5307

Table 5.5: Comparison of dimensionless mass flow due to temperature in terms of rarefaction parameter δ_0 and temperature for polyatomic Nitrogen

		Database Sub. 4.2.1	*[29]*	*Database Sub. 4.2.1*	*[29]*	*Database Sub. 4.2.1*	*[29]*
	δ_0	*300K*		*373.15 K*		*423.15K*	
W_T	*0.01*	0.7205	0.7207	0.7206	0.7208	0.7206	0.7208
	0.1	0.6169	0.6185	0.6174	0.6189	0.6176	0.6190
	0.5	0.4670	0.4717	0.4685	0.4727	0.4692	0.4732
	0.55	0.45660	0.4609	0.4575	0.4620	0.4583	0.4625
	0.60	0.4458	0.4509	0.4474	0.4520	0.4481	0.4525
	0.65	0.4362	0.4415	0.4378	0.4426	0.4386	0.4431
	0.70	0.4272	0.4326	0.4289	0.4338	0.4297	0.4343
	0.75	0.4187	0.4242	0.4204	0.4255	0.4212	0.4260
	1	0.3819	0.3879	0.3838	0.3893	0.3847	0.3899
	1.5	0.3271	0.3335	0.3291	0.3350	0.3300	0.3356
	2	0.2868	0.2932	0.2888	0.2947	0.2897	0.2953
	5	0.1642	0.1690	0.1657	0.1701	0.1664	0.1706
	10	0.0944	0.0974	0.0953	0.0981	0.0958	0.0984
	20	0.0506	0.0523	0.0511	0.0526	0.0513	0.0528
	50	0.0211	0.0218	0.0213	0.0219	0.0214	0.0220

Table 5.5: Continue

		Database Sub. 4.2.1	*[29]*	*Database Sub. 4.2.1*	*[29]*	*Database Sub. 4.2.1*	*[29]*
	δ_0	*573.15K*		*1000K*		*1500K*	
W_T	*0.01*	0.7207	0.7208	0.7207	0.7209	0.7208	0.7209
	0.1	0.6181	0.6194	0.6187	0.6198	0.6190	0.6199
	0.5	0.4705	0.4741	0.4722	0.4752	0.4730	0.4757
	0.55	0.4597	0.4634	0.4615	0.4647	0.4623	0.4652
	0.60	0.4496	0.4535	0.4515	0.4548	0.4523	0.4553
	0.65	0.4402	0.4442	0.4421	0.4454	0.4430	0.4461
	0.70	0.4313	0.4354	0.4332	0.4367	0.4342	0.4373
	0.75	0.4229	0.4271	0.4249	0.4284	0.4258	0.4291
	1	0.3865	0.3911	0.3887	0.3926	0.3897	0.3932
	1.5	0.3319	0.3369	0.3343	0.3384	0.3354	0.3392
	2	0.2916	0.2966	0.2940	0.2982	0.2951	0.2989
	5	0.1678	0.1715	0.1696	0.1728	0.1704	0.1733
	10	0.0967	0.0990	0.0978	0.0998	0.0983	0.1002
	20	0.0518	0.0532	0.0525	0.0536	0.0528	0.0538
	50	0.0216	0.0222	0.0219	0.0223	0.0220	0.0224

In Tables 5.4 and 5.5, the results of the dimensionless mass flow due to pressure and temperature are being compared with [29] from the literature. The results of polyatomic Nitrogen from paragraph 4.2.1 with [29] differ less than than the results of monoatomic Nitrogen with [29].

5.2 Monoatomic Nitrogen gas flow through tapered channels

In many applications, the two vessels are not connected with a cylindrical, fixed-radius tube but with a conical form with increasing radius in the direction of gas flow. In this paragraph 5.2, a method is presented, where the mass flow is calculated for different pressure ratios and inlet rarefaction parameters.

Two vessels are assumed, which are connected with a long tube with variable radius (tapered channel). The pressure and the temperature of the first vessel is P_1 and T_1 respectively. The pressure of the second vessel is $P_2$and its temperature is T_2. The flow rate is given as in [30]:

$$G = \frac{L}{\pi \alpha_I^3 P_I}\left(\frac{2kT_I}{m}\right)^{1/2} \dot{M} \tag{5.3}$$

with α_I being the radius of the tube in vessel 1, k is Boltzmann's constant and M is the mass flow rate through the variable radius tube.

If it is assumed that the length of the tube, L, is much bigger than the biggest radius of the tube, then the mass flow is given as in [30]:

$$\dot{M} = \pi \alpha^2 P \left(\frac{m}{2kT}\right)^{1/2} (-G_P \xi_P + G_T \xi_T) \tag{5.4}$$

where ξ_P, ξ_T are considered as:

$$\xi_P = \frac{a}{P}\frac{dP}{dx} \tag{5.5}$$

$$\xi_T = \frac{a}{T}\frac{dT}{dx} \tag{5.6}$$

with $a = a(x)$ being the local radius of long tube according to longitudinal coordinate and $P = P(x)$ the local pressure respectively.

For $\delta > 50$ the coefficients G_P and G_T, which depend on the value of rarefaction parameter δ, are calculated using the equations from [30]:

$$G_P = \frac{\delta}{4} + \sigma_P \tag{5.7}$$

$$G_T = \frac{\sigma_T}{\delta} \tag{5.8}$$

while $\delta \leq 50$, the value of G_P and G_T is specified from the database presented at [29] for $\omega = 1$.

The parameters σ_P and σ_T are equal to 1.018 and 1.175 respectively, according to the S-model kinetic theory from [31].

The value of the rarefaction parameter is defined as [30]:

$$\delta = \frac{\alpha P}{\mu}\left(\frac{m}{2kT}\right)^{1/2} \tag{5.9}$$

where μ is characterized as the viscosity of the gas.

Redefining the eq. (5.1), the flow rate equation is:

$$G = \frac{L}{P_I}\left(\frac{a}{a_I}\right)^3 \left(\frac{T_I}{T}\right)^{1/2}\left[-G_P(\delta)\frac{dP}{dx} + G_T(\delta)\frac{P}{T}\frac{dT}{dx}\right] \tag{5.10}$$

and the pressure numerically calculated in Jean [20]:

$$P_{i+1} = P_i + \frac{1}{G_P(\delta i)}\left[G_T(\delta_i)\frac{P_i}{T_i}(T_{i+1} - T_i) - GP_i\left(\frac{a_I}{\alpha_i}\right)^3\left(\frac{T_i}{T_I}\right)^{1/2}\frac{\Delta x}{L}\right] \tag{5.11}$$

where $0 \leq i \leq N-1$, $\Delta x = L/N$.

In eq. (5.9), the Pressure at node $i+1$ is calculated numerically and the values of Pressure, Temperature, G_P and G_T are needed to be already specified.

- *ISOTHERMAL FLOW*

It is considered that the gas flow is isothermal, so the temperature in every node is $T(x) = T_1 = T_{stable}$. The radius of the conical tube is given through the function:

$$a(x) = a_I + \frac{x}{L}(a_{II} - a_I) \tag{5.12}$$

where a_I the radius of the tube in vessel 1 and a_{II} the radius of the tube in vessel 2 and the ratio of radius of vessel 1 to vessel 2.

The nodes of z-direction in the algorithm are $N = 90000$. The temperature in Vessel 1 is 300, so in the tube of variable radius and Vessel 1 the temperature is 300. The radius in the first node is 0.005. The reduced flow rate G is calculated as a function of P_{II} and the temporary pressure of the last node of z-direction in every loop until the temporary pressure is equal to P_{II}. In Table 5.6 the results of these calculations for variable inlet δ_0 and pressure ratios are given. Furthermore, these results are compared to the database from [30].

Table 5.6: Comparison of the reduced mass flow for isothermal flow and monoatomic Nitrogen in terms of pressure ratio and the inlet rarefaction parameter

	$P_{II}/P_I = 0$	0.01	0.1	0.5	0.9
δ_0 =0 [30]	27.35	27.08	24.62	13.68	2.735
δ_0 =0	27.3525	27.079	24.6172	13.6768	2.7461
δ_0 =0.01 [30]	27.04	26.76	24.29	13.42	2.672
δ_0 =0.01	26.9909	26.7152	24.2448	13.3947	2.6782
δ_0 =0.1 [30]	25.95	25.67	23.21	12.78	2.547
δ_0 =0.1	25.9388	25.6589	23.2097	12.769	2.5553
δ_0 =1 [30]	25.99	25.73	23.57	13.80	2.910
δ_0 =1	25.9768	25.718	23.563	13.7902	2.9217
δ_0 =10 [30]	52.29	52.17	50.66	35.56	8.531
δ_0 =10	52.2833	52.1610	50.6528	35.5579	8.5727

The results of the reduced flow rate G calculated for tapered channel of 90000 nodes and for isothermal flow, by considering Nitrogen as a monoatomic molecule, are shown on the Table 5.6.

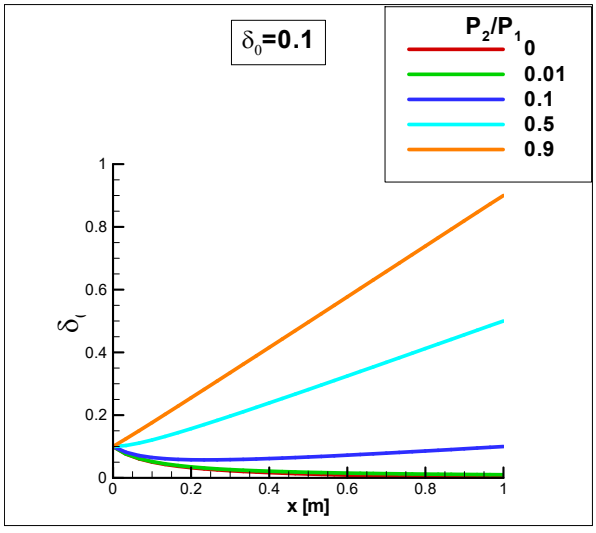

Figure 5.1: δ along x-axis $[\delta_0 = 0.1]$

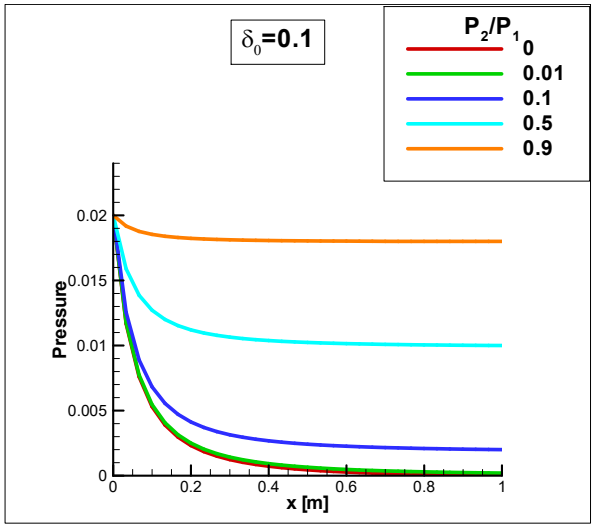

Figure 5.2: Pressure along x-axis $[\delta_0 = 0.1]$

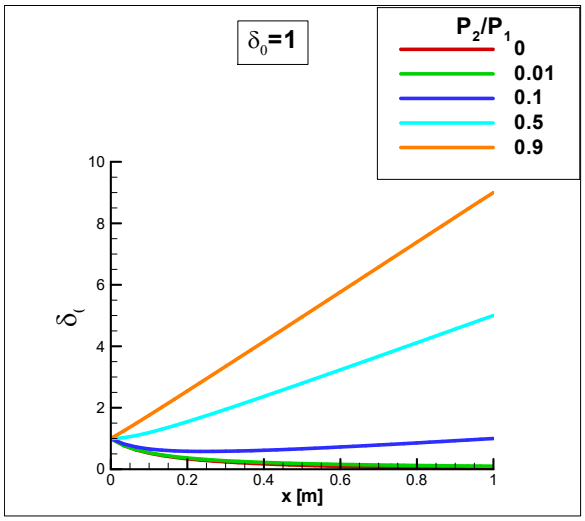

Figure 5.3: δ along x-axis $[\delta_0 = 1]$

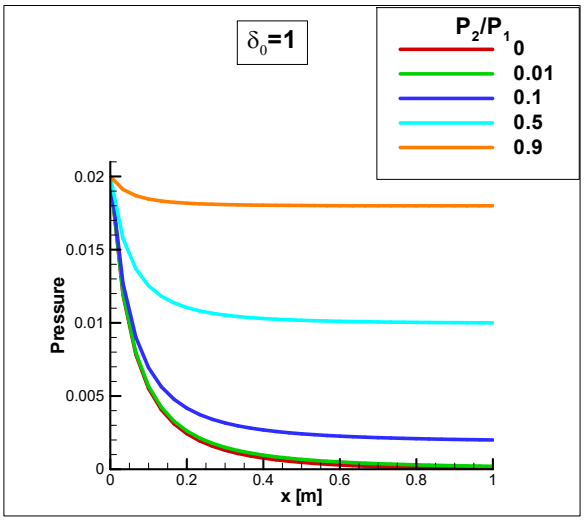

Figure 5.4: Pressure along x-axis $[\delta_0 = 1]$

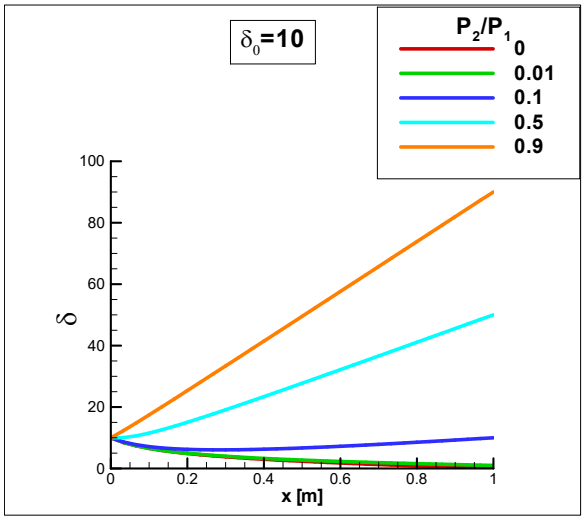

Figure 5.5: δ along x-axis $[\delta_0 = 10]$

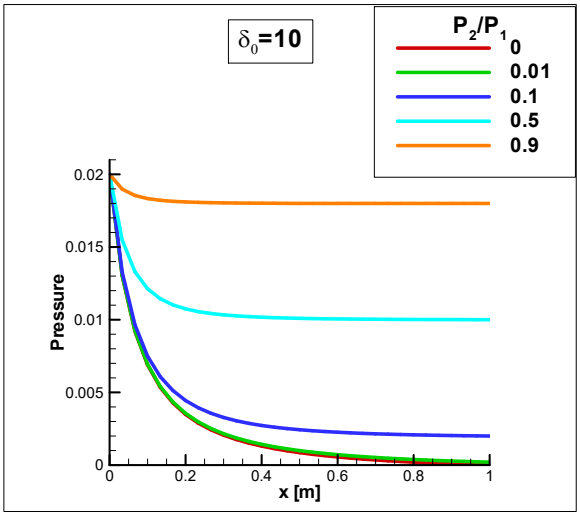

Figure 5.6: Pressure along x-axis $[\delta_0 = 10]$

In Figures 5.1, 5.3 and 5.5 the value of the rarefaction parameter δ along the x-axis of the tapered channel is presented. It is also observed that the value of the rarefaction parameter δ is increasing along the x-axis for higher values of pressure ratios, $P_2/P_1 = 0.9$ and 0.5, while for smaller pressure ratios, $P_2/P_1 = 0$ and 0.01, the value of rarefaction parameter is decreasing. For $P_2/P_1 = 0.1$, the value of rarefaction parameter δ is not changing significantly.

The value of pressure along the x-axis in a tapered channel is being presented on Figures 5.2, 5.4 and 5.6. For smaller pressure ratios, $P_2/P_1 = 0.01$ and 0.1, the value of dimensionless pressure is decreasing rapidly while for pressure ratio $P_2/P_1 = 0.5$ it is decreasing less rapidly

along the x-axis in the tapered channel. It is evident that for a pressure ratio $P_2/P_1 = 0.9$, the value of the dimensionless pressure is not changing significantly.

- *NON-ISOTHERMAL FLOW*

The gas flow is considered to be non-isothermal, so the temperature in every node is:

$$T(x)=T_1 + \frac{x}{L}(T_{II} - T_I) \quad (5.13)$$

The radius of the conical tube is given by eq. (5.12), as in Isothermal flow. The nodes of z-direction in the algorithm are N=90000. The temperature in Vessel 1 is 300K and in Vessel 2 is 78.9K and the temperature in the tube of variable radius can be calculated by eq. (5.13). The radius in the first node is 0.005. The reduced flow rate G is calculated as a function of P_{II} and the temporary pressure of the last node of z-direction in every loop, until the temporary pressure is equal to P_{II}. In Table 5.7 the results of these calculations for variable δ_0 and pressure ratios are given. Furthermore, the results are being compared to the database from [30].

Table 5.7: Comparison of the reduced mass flow for non-isothermal flow and monoatomic Nitrogen in terms of pressure ratio and the inlet rarefaction parameter

	$P_{II}/P_I = 0$	0.01	0.1	0.5	0.9
δ_0 *=0 [30]*	27.35	26.82	22.03	0.7090	-20.61
δ_0 *=0*	27.3525	26.819	22.02	0.6846	-20.648
δ_0 *=0.01 [30]*	27.05	26.51	21.84	2.495	-15.49
δ_0 *=0.01*	26.465	26.465	21.7663	2.4813	-15.5053
δ_0 *=0.1 [30]*	26.00	25.48	21.34	6.526	-6.268
δ_0 *=0.1*	25.9938	25.4722	21.3311	6.4951	-6.3035
δ_0 *=1 [30]*	26.32	25.92	23.26	12.74	1.232
δ_0 *=1*	26.315	25.916	23.2491	12.7196	1.2266
δ_0 *=10 [30]*	54.83	54.73	53.26	37.41	8.818
δ_0 *=10*	54.8192	54.7215	53.2575	37.4267	8.8571

The results of reduced flow rate G calculated for tapered channel of 90000 nodes and for non-isothermal flow, while Nitrogen being considered as a monoatomic molecule, are shown in the Table 5.7.

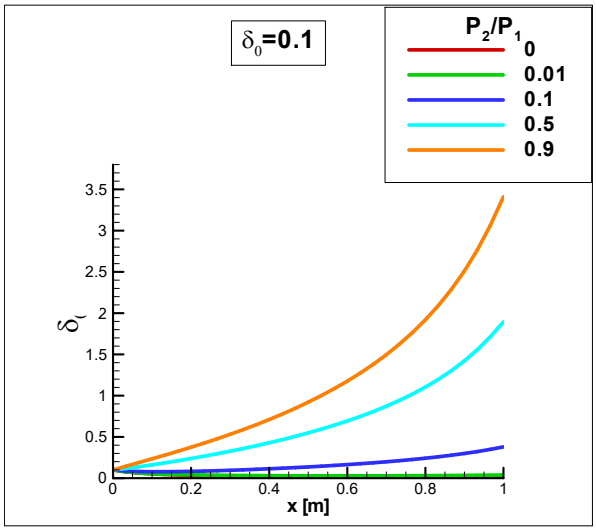

Figure 5.7: δ along x-axis $[\delta_0 = 0.1]$

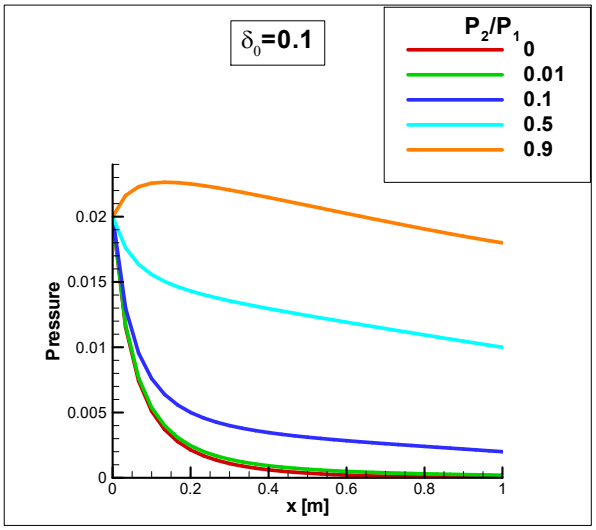

Figure 5.8: Pressure along x-axis $[\delta_0 = 0.1]$

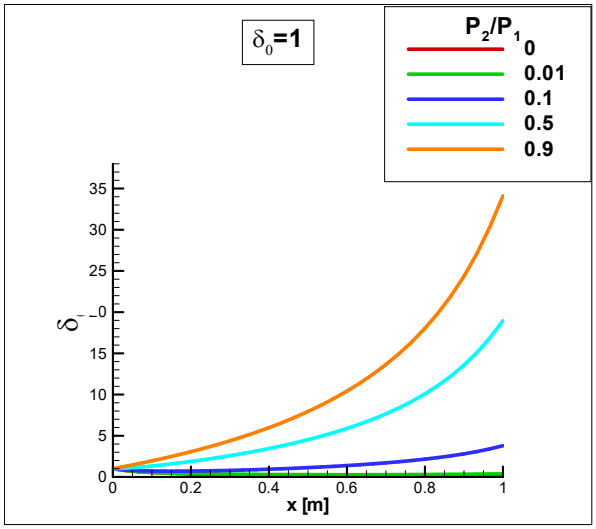

Figure 5.9: δ along x-axis $[\delta_0 = 1]$

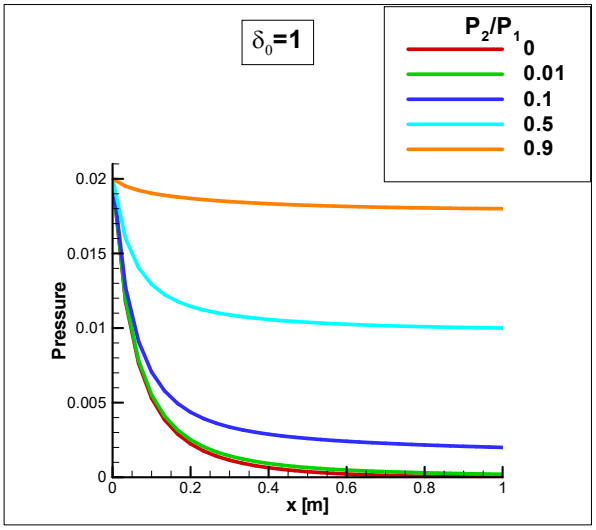

Figure 5.10: Pressure along x-axis $[\delta_0 = 1]$

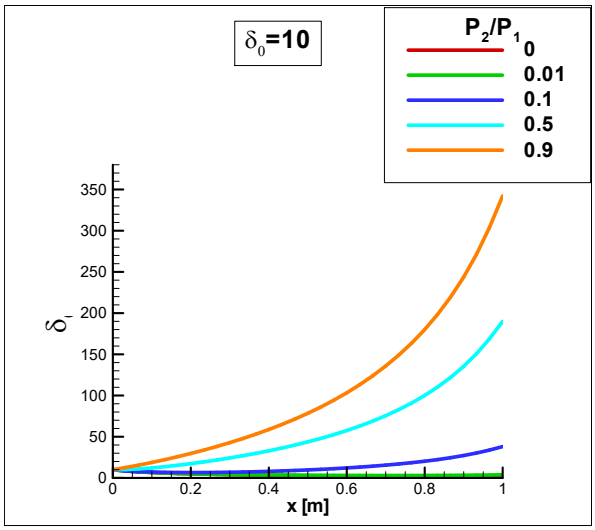

Figure 5.11: δ along x-axis [$\delta_0 = 10$]

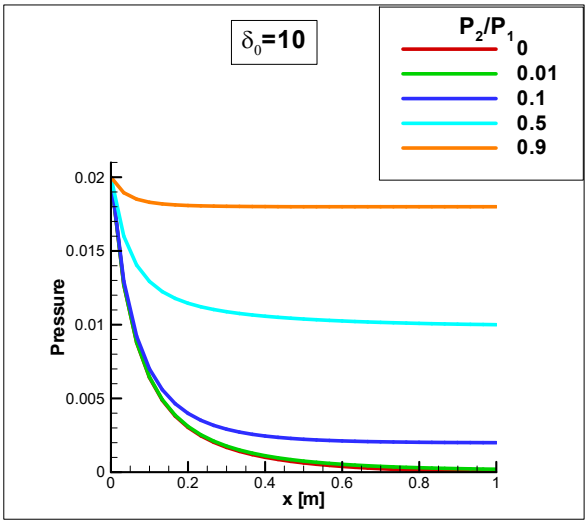

Figure 5.12: Pressure along x-axis [$\delta_0 = 10$]

In Figures 5.7, 5.9 and 5.11 the value of the rarefaction parameter δ along the x-axis of the tapered channel is presented. For small pressure ratios, $P_2/P_1 = 0$ and 0.01, the value of the rarefaction parameter δ is about stable, while for bigger pressure ratios, $P_2/P_1 = 0.1, 0.5\ and\ 0.9$ it is increasing along the x-axis of the tapered channel. It is obvious that for pressure ratios 0.9 and 0.5, the value of rarefaction parameter is increasing rapidly. It is evident that the value of rarefaction parameter δ in non-isothermal flow is almost 3.5 times bigger than in isothermal flow for all the cases of inlet rarefaction parameter δ_0.

The value of pressure along the x-axis in a tapered channel is presented in Figures 5.8, 5.10 and 5.12. The value of the dimensionless pressure along the x-axis in a tapered channel is similar with the value of dimensionless pressure in isothermal flow for inlet rarefaction parameter $\delta = 1$ and 10. On the contrary, for inlet rarefaction parameter δ_0= 0.1, the value of dimensionless pressure is decreasing more rapidly, in contrast with the pressure in isothermal flow. So, it must be noted that the value of pressure for $\delta_0 = 0.1$ and pressure ratio $P_2/P_1 = 0.9$ is increasing approximately in the first 10% of the length of the tapered channel and after that is decreasing.

5.3 Polyatomic Nitrogen gas flow through fixed radius channels

In order to specify the pressure in each node and mass flow, a system of equations is required to be solved. In this case, the gas of Nitrogen is not considered as monoatomic molecule, like in paragraph 5.2, but as a polyatomic molecule.

In monoatomic gases, the value of the parameter $\omega = 1$. But in polyatomic gases, the value of the parameter ω must be set properly. In [18], the following equation is suggested:

$$\omega = 1 + \frac{4\Delta_{rot}}{2\Delta_{rot} - 3} \tag{5.12}$$

The correction to the thermal conductivity interaction of molecular and translational energy is given by Uribe [27] as:

$$\Delta_{rot} = \frac{j\left(2.5 - \frac{\rho D_{rot}}{\mu}\right)}{\pi Z_{rot} + 2\left(\frac{5j}{6} + \frac{\rho D_{rot}}{\mu}\right)} \tag{5.13}$$

In order to solve the equation (5.11), the rotation degrees of freedom need to be specified. For N_2 j=2 and the temperature collision number Z_{rot} can be specified by the eq. (5.2), where Z_{rot}^{∞} can be found from [27]. The reduced temperature $T* = kT_0/\varepsilon$ where ε is the energy scaling factor, can be defined from [27] where the value of expression ε/k is tabulated. The other term that is needed to be specified in order to define Z_{rot} through equation (5.2) is $\rho D_{rot}/\mu$.

The ratio $\rho D_{rot}/\mu$ can be given in two parts according to temperature.

For $T^* \leq T_{cross}^*$

$$\frac{\rho D_{rot}}{\mu} = \frac{Z_{rot}}{(Z_{rot}^{\infty})^{\frac{3}{4}}}\left(1.122 + \frac{4.552}{T^*}\right) \tag{5.14}$$

For $T^* \geq T_{cross}^*$

$$\frac{\rho D_{rot}}{\mu} = \frac{6A^*}{5}\left(1 + \frac{0.27}{Z_{rot}} - \frac{0.44}{{Z_{rot}}^2} - \frac{0.9}{{Z_{rot}}^3}\right) \tag{5.15}$$

where A^* is the ratio of collision integral for viscosity $\Omega^{(2,2)*}$ to collision integral for diffusion $\Omega^{(1,1)*}$. The T_{cross}^* is the reduced crossover temperature as given in [27] and is equal to 6.70 for N_2. The collision integral for viscosity and collision integral for diffusion are defined from the following equations as a function of reduced temperature T^*as being defined in [32].

- $\Omega^{(2,2)*}$

For $1 < T^* < 10$

$$\Omega^{(2,2)*} = \exp\left[0.46641 - 0.56991(lnT^*) + 0.19591(lnT^*)^2 - 0.03879(lnT^*)^3 + 0.00259(lnT^*)^4\right] \quad (5.16a)$$

For $T^* > 10$

$$\Omega^{(2,2)*} = (\rho^*)^2 a^2\left[1.04 + \alpha_1(lnT^*)^{-1} + \alpha_2(lnT^*)^{-2} - \alpha_3(lnT^*)^{-3} + \alpha_4(lnT^*)^{-4}\right] \quad (5.16b)$$

where:

$$a_1 = 0$$

$$a_2 = -33.0838 + (a_{10}\rho^*)^{-2}\left[20.0862 + \left(\frac{72.1059}{a_{10}}\right) + \left(\frac{8.27648}{a_{10}}\right)^2\right]$$

$$\alpha_3 = 0.01571 - (a_{10}\rho^*)^{-2}\left[56.4472 + \left(\frac{286.393}{a_{10}}\right) + \left(\frac{17.7610}{a_{10}}\right)^2\right]$$

$$\alpha_4 = -87.7036 + (a_{10}\rho^*)^{-2}\left[46.3130 + \left(\frac{277.146}{a_{10}}\right) + \left(\frac{19.0573}{a_{10}}\right)^2\right]$$

with $a_{10} = \ln\left(\frac{V_0^*}{10}\right)$ and $a_{10} = \ln\left(\frac{V_0^*}{T^*}\right)$. The values of V_0^* , $\rho^*$and ε/k are 5.308x104, 0.1080 and 98.4 for N_2 respectively as are given from Clifford [32].$\Omega^{(1,1)*}$

For $1 < T^* < 10$

$$\Omega^{(1,1)*} = \exp\left[0.295402 - 0.510069(lnT^*) + 0.189395(lnT^*)^2 - 0.045427(lnT^*)^3 + 0.0037928(lnT^*)^4\right] \quad (5.17a)$$

For $T^* > 10$

$$\Omega^{(1,1)*} = (\rho^*)^2 a^2\left[0.89 + b_2(T^*)^{-2} + b_4(T^*)^{-4} - b_6(T^*)^{-6}\right] \quad (5.17b)$$

where:

$$b_2 = -267.00 + (a_{10}\rho^*)^{-2}\left[201.570 + \left(\frac{174.672}{a_{10}}\right) + \left(\frac{7.36916}{a_{10}}\right)^2\right]$$

$$b_4 = -26700 + (a_{10}\rho^*)^{-2}\left[19.2265 + \left(\frac{27.6938}{a_{10}}\right) + \left(\frac{3.29559}{a_{10}}\right)^2\right] x\ 10^3$$

$$b_6 = -8.90\ x\ 10^5 + (a_{10}\rho^*)^{-2}\left[6.31013 + \left(\frac{10.2266}{a_{10}}\right) + \left(\frac{2.33033}{a_{10}}\right)^2\right] x\ 10^5$$

The procedure of calculating the reduced flow G is the same as in paragraph 5.2 but the value of ω is in the range 0 to 1.

To investigate the flow of polyatomic Nitrogen, the parameter g* must be calculated for temperature ratios $T_2/T_1 = 2$ and $T_2/T_1 = 3$ and for $P_2 = P_1$, in order for the method of calculations to be verified with [29].

In Table 5.8 and 5.9, the results of the calculations are compared with the previous temperature ratios and for fixed radius channel.

Table 5.8: Comparison of the reduced mass flow for polyatomic Nitrogen in terms of the inlet rarefaction parameter for $T_2/T_1 = 2$ and isobaric flow in fixed radius channel

	Tantos [29]	*Shakhov*	*Results*
δ_0 *=0.01*	0.4258	0.426	0.4257
δ_0 *=0.1*	0.3731	0.3745	0.373
δ_0 *=0.5*	0.2924	0.2967	0.2922
δ_0 *=1*	0.2456	0.2513	0.2452
δ_0 *=5*	0.11954	0.1252	0.11924
δ_0 *=10*	0.07274	0.07667	0.07255
δ_0 *=20*	0.04049	0.04281	0.04036
δ_0 *=30*	0.02789	0.02952	0.02779

Table 5.9: Comparison of the reduced mass flow for polyatomic Nitrogen in terms of the inlet rarefaction parameter for $T_2/T_1 = 3$ and isobaric flow in fixed radius channel

	Tantos [29]	*Shakhov*	*Results*
δ_0 *=0.01*	0.6163	0.6165	0.6162
δ_0 *=0.1*	0.5444	0.5461	0.5443
δ_0 *=0.5*	0.438	0.4358	0.4304
δ_0 *=1*	0.3642	0.3709	0.3636
δ_0 *=5*	0.1861	0.1928	0.1854
δ_0 *=10*	0.1176	0.1224	0.1171
δ_0 *=20*	0.06743	0.07034	0.06705
δ_0 *=30*	0.04714	0.0492	0.04685

The comparison Tables 5.8 and 5.9 validates the method that was followed and its calculations. The method is being used in order to calculate the flow of polyatomic Nitrogen in tapered channel for different pressure ratios and temperature ratios as in paragraph 5.2.

5.4 Polyatomic Nitrogen gas flow through tapered channels

In paragraph 5.1 it the reduced mass flow in tapered channel considering Nitrogen as monoatomic gas was investigated. The current analysis considers Nitrogen as a polyatomic molecule. It is necessary to be stated that there is no extensive research for mass flow of rarefied polyatomic Nitrogen in long tapered channels, in contrast with monoatomic Nitrogen, due to its complexity. The results that are presented in this chapter, are being compared with [30] due to the unavailability in the literature of results for rarefied polyatomic Nitrogen for tapered channels.

- *ISOTHERMAL FLOW*

In paragraph 5.3, the method of researching the rarefied polyatomic Nitrogen flow in fixed radius channels was thoroughly presented. In contrast with fixed radius channels, in tapered channels, the radius is not fixed but is specified by eq. (5.12). The parameters of the researching case are the same as for monoatomic Nitrogen. The parameters of the polyatomic Nitrogen are specified as in the paragraph 5.2. The results of the reduced mass flow of polyatomic Nitrogen in tapered channel in isothermal flow is presented in Table 5.10.

The coefficients G_P and G_T depend on the value of rarefaction parameter δ. Their analytical expressions are given as for $\delta > 50$ by:

$$G_P = \frac{\delta}{4} + \sigma_P \tag{5.7}$$

$$G_T = 0.3\frac{1.5}{\delta}\text{ftr} \tag{5.19}$$

where $ftr = \frac{5}{3-\omega}$ and $\sigma_P = 1.1018$

while for $\delta \leq 50$, the value of G_P and G_T is specified from the database from [30].

Table 5.10: Comparison of the reduced mass flow for isothermal flow and polyatomic Nitrogen in terms of pressure ratio and the inlet rarefaction parameter

	$P_{II}/P_I = 0$	0.01	0.1	0.5	0.9
δ_0 =0 [30]	27.35	27.08	24.62	13.68	2.735
δ_0 =0	27.3517	27.0781	24.6165	13.6758	2.7350
δ_0 =0.01 [30]	27.04	26.76	24.29	13.42	2.672
δ_0 =0.01	26.9883	26.7126	24.2424	13.3928	2.6675
δ_0 =0.1 [30]	25.95	25.67	23.21	12.78	2.547
δ_0 =0.1	25.9279	25.6480	23.1984	12.7595	2.5426
δ_0 =1 [30]	25.99	25.73	23.57	13.80	2.910
δ_0 =1	25.9264	25.6674	23.5126	13.7585	2.8996
δ_0 =10 [30]	52.29	52.17	50.66	35.56	8.531
δ_0 =10	52.2295	52.1075	50.6052	35.5367	8.5253

The results of the reduced flow rate G calculated for tapered channel of 90000 nodes and for isothermal flow, while Nitrogen is considered to be a polyatomic molecule, are shown on the Table 5.10. It is obvious that all databases calculated on Chapter 4 are being validated. Differences between the results of the research and the [30] occur due to the precision of calculations due to the fact that the results of the Table 5.10 are for polyatomic Nitrogen while in [30] for monoatomic Nitrogen.

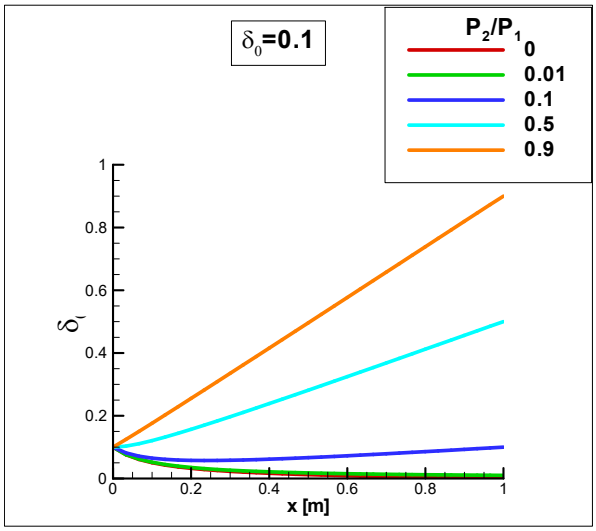

Figure 5.13: δ along x-axis $[\delta_0 = 0.1]$

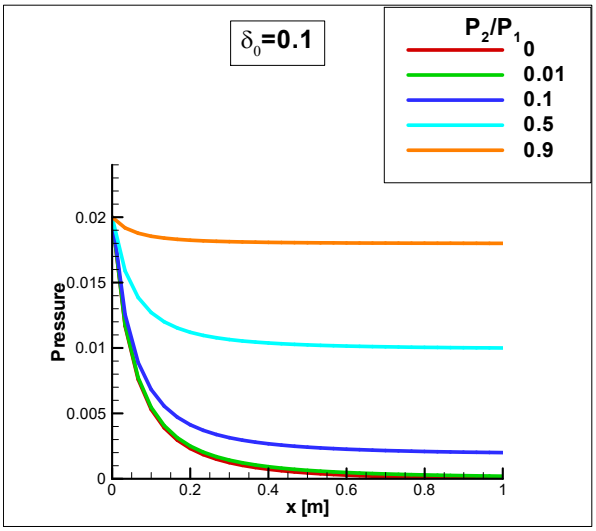

Figure 5.14: Pressure along x-axis $[\delta_0 = 0.1]$

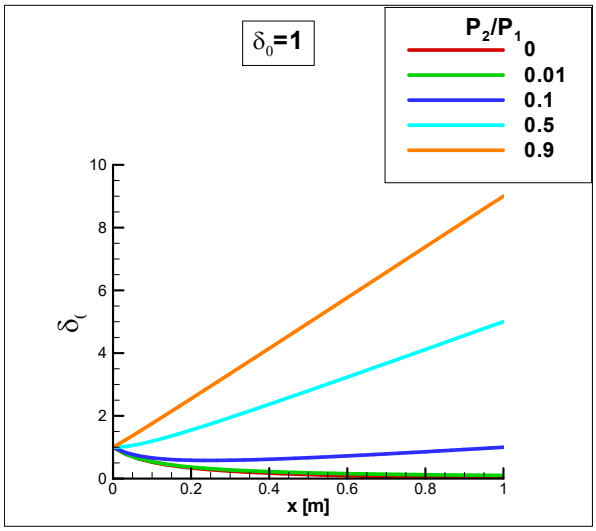

Figure 5.15: δ along x-axis $[\delta_0 = 1]$

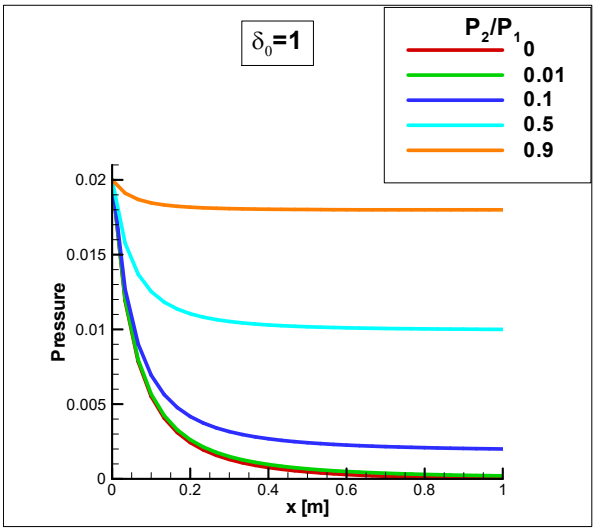

Figure 5.16: Pressure along x-axis $[\delta_0 = 1]$

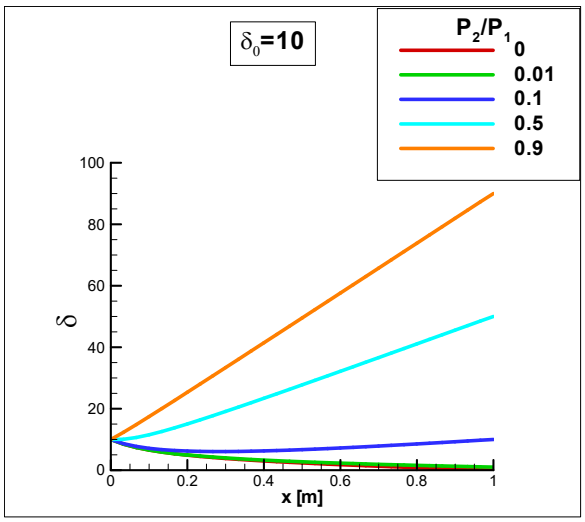

Figure 5.17: δ along x-axis $[\delta_0 = 10]$

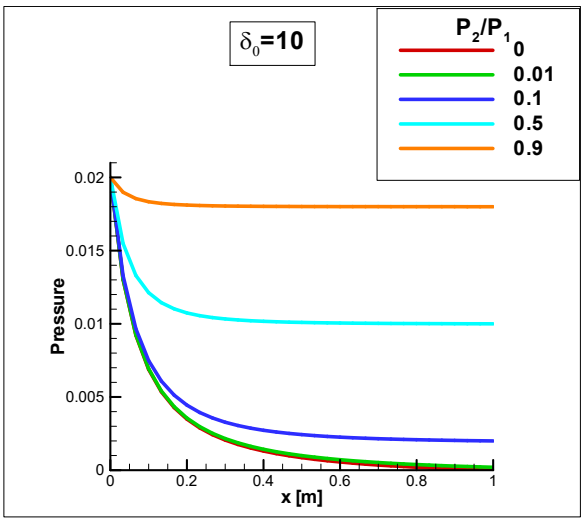

Figure 5.18: Pressure along x-axis $[\delta_0 = 10]$

The Figures 5.13, 5.15 and 5.17 present the value of the rarefaction parameter δ along the x-axis of the tapered channel. Along the x-axis, the dimensional and rarefaction δ values of the tube are almost the same with the values calculated for the monoatomic Nitrogen, where δ_0 is 0.1 or 1 or 10.

The pressure's value along the x-axis in a tapered channel is presented on Figures 5.14, 5.16 and 5.18. For smaller pressure ratios, $P_2/P_1 = 0$, 0.01 and 0.1, the value of dimensionless pressure is rapidly decreasing, while for the pressure ratio $P_2/P_1 = 0.5$ is decreasing at a slower rate along the x-axis in the tapered channel likewise the case of

monoatomic Nitrogen. Also, the dimensional value of the pressure along the x-axis for pressure ratio $P_2/P_1 = 0.9$ is similar with the results of monoatomic Nitrogen.

- *NON-ISOTHERMAL FLOW*

The rarefied polyatomic Nitrogen gas flow through tapered channel, where the temperature of the two reservoirs is different, as described in paragraph 5.2, and are connected with the tapered channel, demand more complex calculations. The coefficients G_P and G_T are calculated as for isothermal flow (polyatomic Nitrogen).

Table 5.11: Comparison of the reduced mass flow for non-isothermal flow and polyatomic Nitrogen in terms of pressure ratio and the inlet rarefaction parameter

	$P_{II}/P_I = 0$	0.01	0.1	0.5	0.9
δ_0 *=0 [30]*	27.35	26.82	22.03	0.7090	-20.61
δ_0 *=0*	27.3515	26.8182	22.0183	0.6856	-20.6472
δ_0 *=0.01 [30]*	27.05	26.51	21.84	2.495	-15.49
δ_0 *=0.01*	26.9967	26.4628	21.8034	2.6276	-15.1182
δ_0 *=0.1 [30]*	26.00	25.48	21.34	6.526	-6.268
δ_0 *=0.1*	25.9853	25.4650	21.3701	6.8351	-5.7435
δ_0 *=1 [30]*	26.32	25.92	23.26	12.74	1.232
δ_0 *=1*	26.2755	25.8821	23.2661	12.8191	1.3548
δ_0 *=10 [30]*	54.83	54.73	53.26	37.41	8.818
δ_0 *=10*	54.7761	54.6802	53.2243	37.4116	8.8325

The results for reduced flow rate G calculated for tapered channel of 90000 nodes and for isothermal flow, while Nitrogen is considered to be a polyatomic molecule, are shown on the Table 5.11. Differences between the results of the research and [30] occur due to the precision of calculations and due to the results from Table 5.11 for polyatomic Nitrogen, while in [30] being for monoatomic Nitrogen.

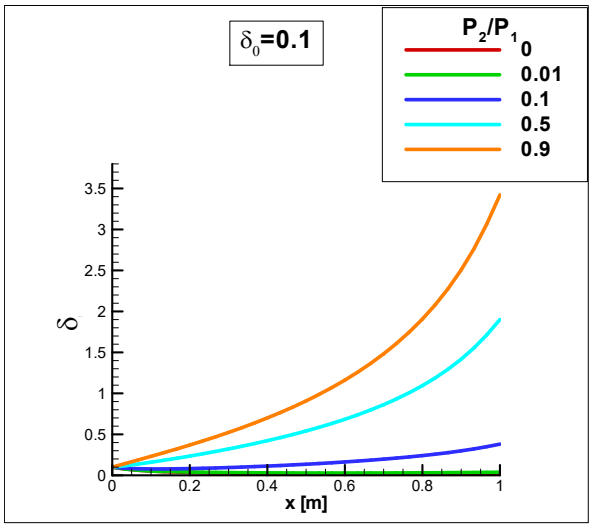

Figure 5.19: δ along x-axis [$\delta_0 = 0.1$]

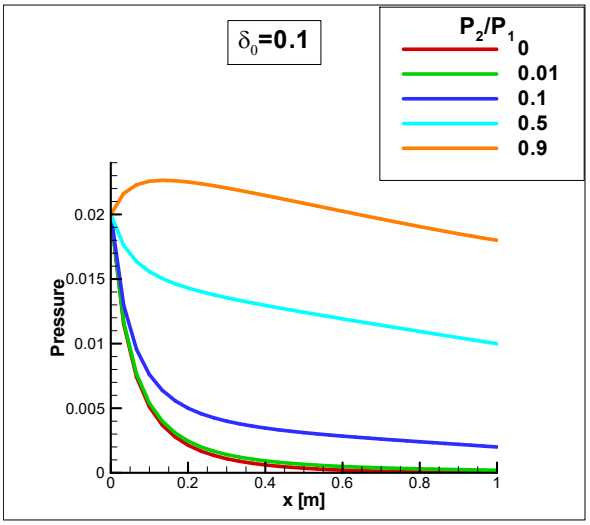

Figure 5.20: Pressure along x-axis [$\delta_0 = 0.1$]

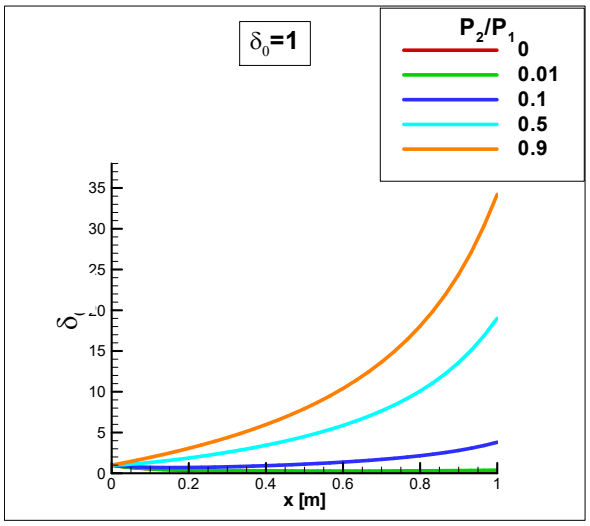

Figure 5.21: δ along x-axis [$\delta_0 = 1$]

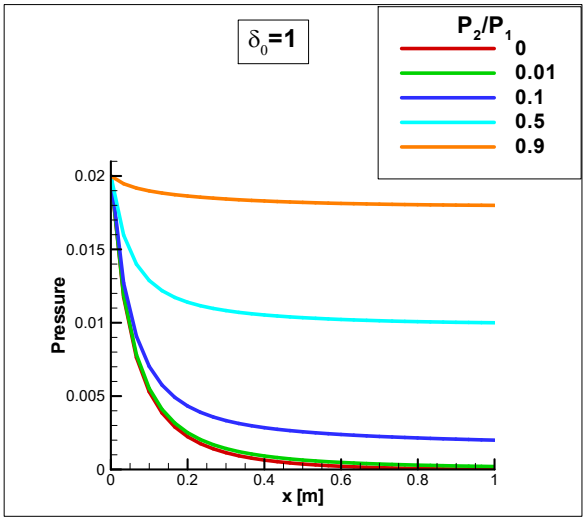

Figure 5.22: Pressure along x-axis [$\delta_0 = 1$]

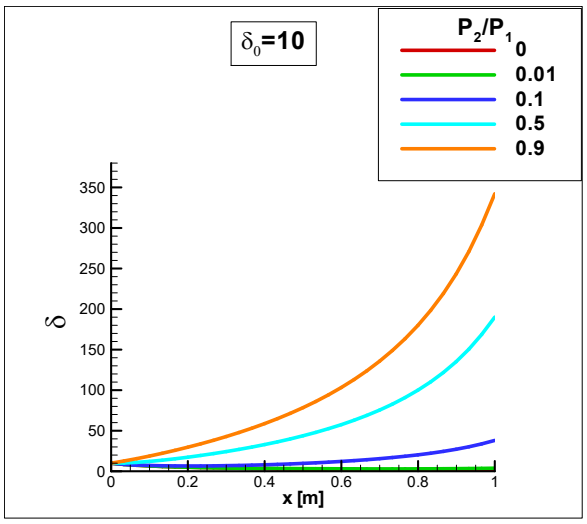

Figure 5.23: δ along x-axis [$\delta_0 = 10$]

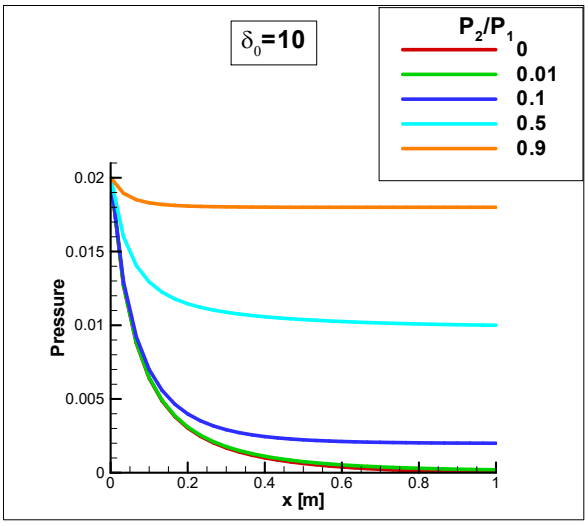

Figure 5.24: Pressure along x-axis [$\delta_0 = 10$]

In Figures 5.19 to 5.24 the rarefaction parameter δ_0 and dimensionless pressure along the x-axis for rarefied polyatomic Nitrogen through long tapered channel for non-isothermal flow is presented. It should be noted that the value of the parameters is similar with the value of the same case flow for monoatomic Nitrogen. Furthermore, it is imperative to be noted that the ftr parameter is used for non-isothermal flow and for polyatomic Nitrogen. In this case, the ftr is calculated when $\delta > 50$ because for rarefaction parameters $\delta \leq 50$, the value of mass flow due to pressure and temperature is derived from [29]. In Figure 2.25, the value of parameter ftr along the x-axis where the value of rarefaction parameter δ was bigger than 50 is presented.

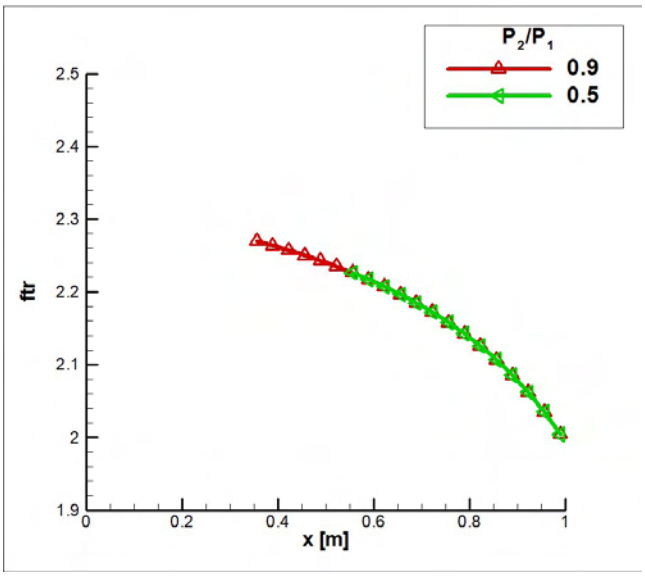

Figure 2.25.: Parameter ftr along x-axis for rarefaction parameter inlet δ_0 and pressure ratios 0.9 and 0.5

Chapter 6. CONCLUSIONS – SUGGESTIONS FOR FURTHER STUDY

6.1 Concluding Remarks

In the current Thesis, the rarefied polyatomic flow of Nitrogen through long tapered channels and long cylindrical (fixed radius) tubes is investigated. In the flows under consideration a wide range of temperature (300 K to 1500 K) and rarefaction parameters is used.

The gas flow in this type of applications cannot be described by the Navier-Stokes equations, so it is being described through the Boltzmann's equation based on the Rykov model. The Rykov model demands the determination of many parameters. The specification of these parameters is accomplished by two different methods using the theoretical analysis by Mason and Monchick [1]. In the first method, the Prandtl of the gas is provided by bibliography [27]. The determination of the other parameters, more precisely the parameters ω_0 and ω_1, is completed as a function of Prandtl Number. In contrast, the specification of these two parameters is determined the theoretical analysis of Mason and Monchick [1] which is extensively described in Chapter 4. The comparison of the results of these two methods conclude to the fact that there is no significant difference among them. This can be applied in both industrial and research sectors. The databases presented provide information and results for a circular cross-section in a long tube for a wide range of temperatures, Prandtl numbers, rarefaction parameters and radius, as the results are dimensionless. The databases that were constructed are verified by existing literature.

The main subject of the current thesis is the research of the rarefied polyatomic gas through long tapered channels. There is extensive research in the literature for polyatomic molecules in tapered channels and also for different cross-sections. The flow is investigated for both isothermal and non-isothermal conditions and for a wide range of pressure ratios. In the first case, the Nitrogen is assumed to be a monoatomic molecule while in the second case it is assumed to be a polyatomic molecule.

The databases that were obtained in the current Thesis can be used in order to specify the dimensional results in fixed radius tubes and tapered channels in many applications. Typical examples include the design of gas distribution systems and vacuum pumps.

6.2 Future Work

In the current Thesis, the collision term of Boltzamann ‘s equation was substituted by Rykov ‘s kinetic model. The substitution of other kinetic models would result in different results. The comparison of the results from the use of different kinetic models is highly recommended. The advantages and disadvantages of each kinetic model would be noted.

The database, that was developed for a wide range of temperature and rarefaction parameters provides the capability to research many long channels with fixed and variable radius, converging and diverging for different pressure ratios, different temperature ratios and radius ratios between the two edges of the channel.

The current Thesis is focused on the research of the N_2. The databases and the methods which are provided in this Thesis can be used in order to research the flow, in variable and fixed radius, of other gases as SF_6, CO_2 and CH_4.

The investigation of gas flows through various cross section should not be limited in coaxial radius tubes. Parallel plates, trapezoidal, triangular and rectangular cross sections can be found in many industrial applications.

REFERENCES

[1] E. A. Mason and L. Monchick, *Heat conductivity of polyatomic and polar gases*, The Journal of Chemical Physics, 36(6), 1622-1639, 1962.

[2] M. Knudsen, *Die Molekularstroemung der Gase durch Offnungen und die Effusion*, Annalen der Physik, 333(5), 999-1016, 1909.

[3] C. S. Wang-Chang and G. E. Uhlenbeck*, Transport phenomena in polyatomic gases, University of Michigan Engineering*, Research Report CM-681, 1951.

[4] C. A. Brau, *Kinetic theory of polyatomic gases models for collisions processes*, Physics of Fluids, 10(1), 48-55, 1967.

[5] Ohwada T, Sone Y, Aoki K, *Numerical analysis of the Poiseuille and thermal transpiration flows between two parallel plates on the basis of the Boltzmann equation for hard-sphere molecules*, Phys Fluids A 1:2042–2049, 1989

[6] Sharipov F, Seleznev V, *Data on internal rarefed gas fows*, J Phys Chem Ref Data 27:657–706, 1989

[7] S. K. Loyalka and T. S. Storvick*, Kinetic theory of thermal transpiration and mechanocaloric effect. III. Flow of a polyatomic gas between parallel plates*, J. Chem. Phys. 71, 339,1979

[8] S. K. Loyalka, T. S. Storvick and S.S. Lo, *Thermal transpiration and mechanocaloric effect. IV. Flow of a polyatomic gas in a cylindrical tube*, J. Chem. Phys. 76, 4157,1982

[9] L. Boltzmann, Weitere studien ber das wrmegleichgewicht unter gasmoleklen, Sitzung Berichte Kaiserl. Akad. der Wissenschaften, 66(2), 275370, 1872.

[10] L. Wu, C. White, T. J. Scanlon, J. M. Reese and Y. Zhang*, A kinetic model of the Boltzmann equation for non-vibrating polyatomic gases*, Journal of Fluid Mechanics, 763, 24-50, 2015.

[11] V. A. Rykov and V. N. Skobelkin*, Macroscopic description of the motions of a gas with rotational degrees of freedom*, Fluid Dynamics, 13(1), 144-147, 1978.

[12] L. H. Holway, *New statistical models for kinetic theory: Methods of construction, Physics of Fluids,* 9(9), 1658-1673, 1966.

[13] C. Day and D. Murdoch, *The ITER Vacuum Systems*, Journal of Physics: Conference Series, 114, 2008.

[14] W. P. Wood, *Kinetic theory analysis of light scattering in polyatomic gases*, Australian Journal of Physics, 24, 555567, 1971.

[15] F. J. McCormack, *Construction of linearized kinetic models for gaseous mixtures and molecular gases*, Physics of Fluids, 16(12), 2095-2105, 1973.

[16] V. A. Rykov*, A model kinetic equation for a gas with rotational degrees of freedom, Fluid Dynamics*, 10(6), 956-966, 1975.

[17] P. Andries, P. L. Tallec, J. P. Perlat and B. Perthame, *The Gaussian-BGK model of Boltzmann equation with small Prandtl number*, European Journal of Mechanics B/Fluids, 19(6), 813-830, 2000.

[18] W. Marques Jr., *Light scattering and sound propagation in polyatomic gases with classical degrees of freedom*, Continuum Mechanics and Thermodynamics, 16(6), 517528, 2004.

[19] A. S. Fernandes and W. Marques Jr., *Kinetic model analysis of time-dependent problems in polyatomic gases*, Phusica A, 373, 97-118, 2007

[20] J. Jean*, An Introduction to the Kinetic Theory of Gases*, Cambridge University Press,1967.

[21] F. Sharipov and V. Seleznev, *Data on internal rarefied gas flows*, Journal of Physical and Chemical Reference Data, 27(3), 657-706, 1998.

[22] V. A. Titarev and E. M. Shakhov, *Poiseuille Flow and Thermal Creep in a Capillary*

[23] C. Tantos, *Effect of rotational and vibrational degrees of freedom in polyatomic gas heat transfer, flow and adsorption processes far from local equilibrium,* Degree of Doctor of Philosophy,152-157, 2016

[24] J. C. Maxwell, *The Scientific Papers of James Clerk Maxwell*, Cambridge University Press, London, 1890

[25] M. Knudsen, *Thermischer Molekulardruck der Gase in Rhren*, Annalen der Physik, 338(16), 1435-1448, 1910.

[26] O. Reynolds, *On certain dimensional properties of matter in the gaseous state*. Part I and Part II, Royal Society Publishing, 170, 727, 1880.

[27] F. J. Uribe, E. A. Mason, and J. Kestin, *Thermal Conductivity of Nine Polyatomic Gases at Low Density*, Journal of Physical and Chemical Reference Data 19, 1123,1990

[28] EES

[29] C. Tantos, *Polyatomic thermal creep flows through long microchannels at large temperature ratios,* Journal of Vacuum Science & Technology A 37, 051602,2019

[30] F. Sharipov, G. Bertoldo, *Rarefied gas flow through a long tube of variable radius,*2005

[31] F. Sharipov, Eur. J. Mech. B/Fluids 22, 133,2003

[32] A. A. Clifford, J. Kestin, and. W. A. Wakeham, Physica A97, 287,1979

[33] E. M. Shakhov, *Generalization of the Krook kinetic relaxation equation*, Fluid Dynamics, 3(5), 95-95, 1968.

[34] F. Sharipov, *Rarefed gas fow through a long tube at any temperature ratio.* J Vac Sci Technol A 14:2627–2635, 1996.

[35] I. Graur, F. Sharipov, *Non-isothermal flow of rarefied gas through a long pipe with elliptic cross section.* Microfuid Nanofuid 6:267–275, 2009

[36] AA Alexeenko, SF Gimelshein, EP Muntz, AD Ketsdever, *Kinetic modeling of temperature driven fows in short microchannels*. Int J Therm Sci 45:1045–1051, 2006

[37] S. Pantazis, S. Naris, C. Tantos, D. Valougeorgis, J. Andre, F. Millet, JP. Perin, *Nonlinear vacuum gas flow through a short tube due to pressure and temperature gradients*. Fusion Eng Des 88:2384–2387, 2013

[38] F. Sharipov*, Non-isothermal gas fow through rectangular microchannels*. J Micromech Microeng 9(4):394–401, 1999

[39] K. Ritos, Y. Lihnaropoulos, S. Naris, D. Valougeorgis, *Pressure and Temperature-driven flow through triangular and trapezoidal microchannels.* Heat Transf Eng 32(13–14):1101–1107, 2011